Helsinki University of Technology Publications in Engineering Physics

Teknillisen korkeakoulun teknillisen fysiikan julkaisuja

Espoo 2005 TKK-F-A838

LASER-INTERFEROMETRIC ANALYSIS OF SURFACE ACOUSTIC WAVE RESONATORS

Jouni Knuuttila

Dissertation for the degree of Doctor of Science in Technology to be presented with due permission of the Department of Engineering Physics and Mathematics for public examination and debate in Auditorium TU1 at Helsinki University of Technology (Espoo, Finland) on the 3rd of June, 2005, at 12 noon.

Helsinki University of Technology
Department of Engineering Physics and Mathematics
Materials Physics Laboratory

Teknillinen korkeakoulu
Teknillisen fysiikan ja matematiikan osasto
Materiaalifysiikan laboratorio

Distribution:
Helsinki University of Technology
Department of Engineering Physics and Mathematics
Materials Physics Laboratory
P.O. Box 2200
FI-02015 TKK
Tel. +358-9-451-5600
Fax. +358-9-451-3164
E-mail: adent@focus.hut.fi

ISBN 951-22-7698-4
ISBN 951-22-7699-2 (PDF)
ISSN 1456-3320
ISSN 1459-7268 (PDF)
URL: http://lib.tkk.fi/Diss/2005/isbn9512276992/

TKK-F-A838

Otamedia Oy
Espoo 2005

HELSINKI UNIVERSITY OF TECHNOLOGY
P.O. BOX 1000, FI-02015 TKK
http://www.tkk.fi

ABSTRACT OF DOCTORAL DISSERTATION

Author Jouni Veikko Knuuttila

Name of the dissertation
Laser-Interferometric Analysis of Surface Acoustic Wave Resonators

Date of manuscript 22 March 2005 | Date of the dissertation 3 June 2005

☐ Monograph ☑ Article dissertation (summary + original articles)

Department Engineering Physics and Mathematics
Laboratory Materials Physics Laboratory
Field of research Interferometric imaging and analysis of surface acoustic waves and devices
Opponent(s) Prof. Helge E. Engan
Supervisor Prof. Matti Kaivola
(Instructor) Prof. Martti M. Salomaa

Abstract
The research work described in this Thesis concentrates on studying surface acoustic wave (SAW) resonators, in particular resonators which utilize the leaky surface acoustic wave (LSAW) mode. Such resonators constitute building blocks for radio-frequency SAW bandpass filters, which are widely employed in modern cordless and cellular telecommunication systems. The number of radio frequency SAW filters produced presently exceeds 3 billion per year.

The work is carried out with an optical Michelson laser interferometer developed at the Materials Physics Laboratory specifically for the purpose of studying SAW components. In the course of this work the interferometer was equipped with a high-speed photodetector and state-of-the-art detection electronics, enabling the measurement of surface vibrations at frequencies as high as 2 GHz with amplitudes on the order of a few picometers. Furthermore, the setup was equipped with high-precision motorized scanning stages and computer control in order to facilitate automatically performed two-dimensional scans with a large number of scanning points and measuring speeds up to 50 000 points per hour. The optical setup features a spatial resolution better than one micrometer, enabling measurement of surface waves with wavelengths down to 2 micrometers. The interferometer can be used for analysis of surface acoustic wave devices as well as for thin-film bulk acoustic wave resonators and radio-frequency microelectromechanical systems (RF-MEMS).

Laser-interferometric measurements were performed on LSAW resonators and filters on rotated Y-cut lithium tantalate (LiTaO3). As a result, an unexpected acoustic field distribution was observed. Further measurements and simulations showed that the observed field distributions resulted from LSAWs escaping outside the resonator into the busbars. This acoustic loss mechanism can significantly degrade the performance of an LSAW filter. The obtained results have been acknowledged by SAW filter manufacturers in Japan and in Europe. In addition, measurements of bulk acoustic wave (BAW) radiation from LSAW resonators were carried out. Such radiation is inherent for LSAW resonators. Theoretical models and numerical simulations characterizing the phenomenon exist but very few direct measurements have been reported. Here, direct measurement results of BAW radiation fields generated by an LSAW resonator on LiTaO3 are reported revealing both fast shear and slow shear bulk waves. Furthermore, two coupling mechanisms, backscattering and direct excitation, were identified. Such information can be used in the development of more accurate simulation models.

Keywords leaky surface acoustic waves, bulk acoustic waves, LSAW resonator, laser interferometry, acoustic losses

Number of pages	46 p. + app. 10 p.	ISBN (printed)	951-22-7698-4
ISBN (pdf)	951-22-7699-2	ISBN (others)	
ISSN (printed)	1456-3320	ISSN (pdf)	1459-7268

Publisher Helsinki University of Technology, Materials Physics Laboratory

Print distribution

☑ The dissertation can be read at http://lib.tkk.fi/Diss/ 2005/isbn9512276992/

Preface

All the research for this dissertation was carried out in the Materials Physics Laboratory at Helsinki University of Technology. Significant part of the work was done in collaboration with Micronas Semiconductor SA, Neuchâtel, Switzerland and with Thomson Microsonics (currently TEMEX), Sophia-Antipolis, France. My work has been financially supported by the Nokia Foundation and the Foundation of Technology (TES, Finland) through scholarships and a travel grant. I would also like to thank the graduate school in Technical Physics for accommodating my graduate studies and research.

I miss Professor Martti M. Salomaa, the director of the Materials Physics Laboratory. His untimely death on the 9^{th} of December 2004 deprived an inspiring and talented instructor from me as well as from many other students. Professor Salomaa was my steadfast supervisor from the very beginning of my work at the University and I remain indebted to him for his persistent support over the past eleven years. His efforts for organizing the resources for the experimental part of this work were extraordinary and his trust and encouragement indispensable, first for the completion of my Master's thesis and later on during my PhD work. His enthusiasm and devotion towards science were inspiring for a young researcher. I was fortunate–and privileged–to work in his laboratory. In future I hope to keep up the same joyful attitude towards work and new challenges as Martti did.

The experimental results achieved with the laser interferometer would probably have amounted to very little without the contributions of Dr. Clinton Hartmann, Professor Viktor Plessky and Dr. Julius Koskela. The insight of Dr. Hartmann and Professor Plessky on surface acoustic waves and the diligent simulation work of Dr. Koskela helped to explain the acoustic leakage effect observed experimentally. I am deeply grateful to all three for harnessing their knowledge and expertise to interpret the cryptic wave field patterns time and again. With such outstanding scientists as co-authors it is practically impossible to fail. I would especially like to thank Dr. Hartmann for providing the idea of studying bulk acoustic wave radiation on the backside of the substrate. The followed research gave birth to two of the seven publications constituting my Thesis work.

I also wish to credit Dr. Thor Thorvaldsson. When the interferometer was ready to be tested with real-life SAW components, the first samples were provided by him and his colleagues at Micronas Semiconductor SA. These samples were crucial for perfecting the setup and played an important role in the discovery of the banana effect. Pasi Tikka is acknowledged for his help in developing the interferometer during the early years and Maria Huhtala is acknowledged for doing measurements and programming the first visualization software. Furthermore, I want to thank Jaakko Saarinen for carrying out measurements and Juha Vartiainen for developing the fast visualization program still in use as well as for devising several data analysis tools.

Collaboration–in the framework of Eureka project E! 2442 SUMO–with people from Temex Microsonics was not only scientifically fruitful but also a very pleasant period of intensive teamwork and mutual visits between the groups. I wish to express my whole-hearted thanks to William Steichen, Marc Solal, Laurent Kopp and Stéphane Chamaly. I also wish to thank Pierre Dufilie, from Temex USA, for sharing his insight on fan-shaped filters. Over the years I have also enjoyed many interesting and enlightening discussions with people working in the field: Professors Ken-ya Hashimoto, Ali-Reza Baghai-Wadhi, Takao Chiba and Dr. Clemens Ruppel. Thank you for teaching a novice like me.

I am delighted that so many members of the surface acoustic wave group are present at the laboratory at the time of my dissertation. Very special thanks go to Tapani Makkonen who was always ready to lend me an ear whenever I was facing problems, both in the office as well as off-duty. I value his friendship very much. I also want to thank Saku Lehtonen for being the positive force of the laboratory amidst challenging times, and especially for helping me and others after the departure of Prof. Salomaa. Without Saku's encouragement, proofreading and guidance, keeping up with the schedule and, ultimately, completing the manuscript would have been in grave danger. I shall remain indebted to both Saku and Tapani for helping me on numerous occasions when the tangled dissertation process was about to overwhelm me. For many years I was fortunate to have Johanna Meltaus as my roommate, her positive attitude and sense of humor made daily work a joy; [illegible] [illegible]. The next generation of lumberjacks, Olli Holmgren and Kimmo Kokkonen, I thank for pushing the performance of the existing laser interferometer–as well as the boundaries of indecent humor–farther than what I could ever imagine. My consolation is the fact that both scoundrels will some day be tormented with the task of coming up with witty phrases for the prefaces of their PhD books. Finally, I wish to thank all the staff–former and present–at the Materials Physics Laboratory. The atmosphere at the lab has been quite unique and I cannot imagine a better place for carrying out research and daily work.

The members of the academic culinary club, initiated by Drs. Tapani Makkonen and Pekka Äyräs, including in addition Drs. Janne Salo and Teemu Pohjola, cannot–at least with a straight face–be acknowledged for improving my cooking skills. Instead, a big thanks goes out for arranging many delicious culinary moments accompanied with laughter and hilarious blunders with overly complex food recipes.

As for late night nourishment, often vital for the completion of conference papers, thesis work and manuscripts, I owe a big thanks to the staff of the nearby grill located at the Otaniemi mall. They serve the best hamburgers in the metropolitan area–and best of all, upon request, with plenty of extra mayonnaise.

Finally, I would like to thank my friends–including those already mentioned–and my parents for all the support and love that I have received over the years. I am also fortunate to have two top class brothers, Tauno and Lauri. Thanks for being there, dudes! And a warm thanks to Cindy for her encouragement. Sweetie–I finally finished the damned book!

List of Publications

This dissertation is a review of the author's work in the field of surface-acoustic wave technology. It consists of an overview and the following selection of publications in this field:

I J. V. Knuuttila, P. T. Tikka, and M. M. Salomaa, "Scanning Michelson interferometer for imaging surface acoustic wave fields", *Optics Letters* **25**, 613–615 (2000).

II J. V. Knuuttila, P. T. Tikka, C. S. Hartmann, V. P. Plessky, and M. M. Salomaa, "Anomalous asymmetric acoustic radiation in low-loss SAW filters", *Electronics Letters* **35**, 1115–1116 (1999).

III J. Koskela, J. V. Knuuttila, P. T. Tikka, C. S. Hartmann, V. P. Plessky, and M. M. Salomaa, "Mechanism for acoustic leakage in surface-acoustic wave resonators on rotated Y-cut lithium tantalate substrate", *Applied Physics Letters* **75**, 2683–2685 (1999).

IV T. Makkonen, S. Kondratiev, V. P. Plessky, T. Thorvaldsson, J. Koskela, J. V. Knuuttila, and M. M. Salomaa, "Surface acoustic wave impedance element ISM duplexer: modeling and optical analysis", *IEEE Transactions on Ultrasonics, Ferroelectrics, and Frequency Control* **48**, 652–665 (2001).

V J. Koskela, J. V. Knuuttila, T. Makkonen, V. P. Plessky, and M. M. Salomaa, "Acoustic loss mechanisms in leaky SAW resonators on lithium tantalate", *IEEE Transactions on Ultrasonics, Ferroelectrics, and Frequency Control* **48**, 1517–1526 (2001).

VI J. V. Knuuttila, J. Saarinen, C. S. Hartmann, V. P. Plessky, and M. M. Salomaa, "Measurement of BAW radiation from low-loss LSAW resonators", *Electronics Letters* **37**, 1055–1056 (2001).

VII J. V. Knuuttila, J. J. Vartiainen, J. Koskela, V. P. Plessky, C. S. Hartmann, and M. M. Salomaa, "Bulk-acoustic waves radiated from low-loss surface-acoustic-wave resonators", *Applied Physics Letters* **84**, 1579–1581 (2004).

Throughout the overview, these publications are referred to by their Roman numerals.

Author's Contribution

The studies in this dissertion are the result of work carried out in the Materials Physics Laboratory at Helsinki University of Technology (TKK) during the years 1998–2004. Papers II–IV were prepared in collaboration with Micronas Semiconductor SA, Bevaix, Switzerland, while Paper V involved cooperation with Thomson Microsonics, France. Papers VI and VII resulted from discussions with Clinton S. Hartmann, RF SAW Components, Dallas, Texas, USA.

The author has substantially contributed to the research in Papers I–VII. Papers I, II, VI and VII were written by the author with the exception of the theory part of Paper VII. The author actively participated in the writing of Paper IV. All laser-interferometric measurements for Papers I, III, IV and V were planned and carried out by the author. Laser-interferometric measurements for Papers II, VI and VII were proposed and supervised by the author and carried out by the author together with collaborators. Illustrations involving laser-interferometric data for Papers I–VII were prepared by the author.

The author has been responsible for building and developing the scanning Michelson interferometer used for measurements in Publications I–VII. However, many people have contributed to smaller sections such as enhancements to software, electronics and RF shielding. The first optical setup for fixed-spot measurements was constructed during 1995–1996 by Simo Sääskilahti.

The majority of the results covered in Papers I–VII has been presented in international conferences, the results in Papers I, II, VI and VII by the author and those in Papers III, IV and V by the author and collaborators.

List of Abbreviations

The following abbreviations are used in the overview:

BAW	Bulk acoustic wave
COM	Coupling of modes
CRF	Coupled resonator filter
FBAR	Thin-film bulk acoustic wave resonator
GPIB	General-purpose interface bus
IDT	Interdigital transducer
IEF	Impedance element filter
IF	Intermediate frequency
LAN	Local area network
$LiNbO_3$	Lithium niobate
$LiTaO_3$	Lithium tantalate
LSAW	Leaky surface acoustic wave
RF	Radio frequency
RF-MEMS	Radio frequency microelectromechanical systems
Rx	Receiver
SAW	Surface acoustic wave
SSBAW	Slow shear bulk acoustic wave
TCF	Transversely coupled resonator filter

Contents

1 Introduction

Surface acoustic waves (SAWs) are elastic waves propagating on the surfaces of solid media. The term surface acoustic wave originates from the fact that, contrary to bulk waves with a low degree of localization, the surface-wave amplitude attenuates exponentially as a function of depth into the substrate. The most widely known type of SAWs is referred to as a Rayleigh wave after Lord Rayleigh who in 1885 published the first paper with a mathematical solution describing a surface acoustic wave [1]. In nature, surface acoustic waves are observed, along with bulk acoustic waves, in connection with earthquakes.

Surface acoustic waves have been utilized in electronic signal processing since the 1960s. Work on practical applications began in 1965 when White and Voltmer at the University of California developed the interdigital transducer (IDT) which enables the generation of surface acoustic waves via electric excitation on piezoelectric crystals [2]. The electronics industry quickly recognized that signal processing utilizing SAWs could readily be applied to the design of analog electrical filters and delay lines operating at selected frequencies in the range from about 10 MHz up to hundreds of megahertz. Since the early days, SAW technology has found many commercial applications. SAW devices are used in several areas of intermediate and radio-frequency signal processing, including cheap mass-produced filters–numbering in billions of units–used for analog and digital television receivers and remote garage openers. At the other extreme of applications, SAW technology can be found in high-cost, high-performance pulse compressors used for radar applications, as well as in other demanding applications of electronic warfare.

Reasons explaining the success of SAW technology are many. First, SAW devices can be produced using planar semiconductor fabrication technologies. Typically only one or two lithographic steps are required, which makes them cost-competitive in mass-volume applications. Second, SAW devices typically achieve better performance than components implemented with lumped elements. This can be partly attributed to the fact that fairly simple IDT structures can be designed to provide powerful analog signal processing functions, resulting in an excellent performance, e.g., in filtering. Third, SAW components are of small size and light weight. This stems from the slow velocity of surface acoustic waves. In general, a resonating structure will require dimensions of the order of wavelength. For electromagnetic waves propagating at the speed of light the wavelength at 1 GHz is 30 cm. For surface acoustic waves propagating at velocities around 3 km/s, the wavelength is only $\sim$3 μm at the same frequency. The velocity-difference factor of 10^5 is substantial. Although the size of electromagnetic resonator structures can be decreased by using dielectric materials, the extremely small characteristic size provided by surface acoustic waves has not been matched. However, it should be noted that even if a small device size is desirable for applications, the available fabrication technologies set limits to the cost-efficiently

realizable detail size. Hence, very high frequency applications, close to and above 10 GHz, are currently not produced using SAW technology.

The most recent and also perhaps the most challenging applications for surface acoustic wave filters are found in modern wireless communication systems, especially in handheld mobile phones. To fulfill the extremely stringent demands on size and low losses, a novel class of surface-acoustic wave (SAW) filters was developed during the 1980s and 1990s. Simultaneously, to satisfy the requirements set by the then emerging mobile phone standards, such as GSM and PCN, the frequency range for SAW filters was also extended to 1 GHz and later to 2 GHz. Improvements in the achievable resolution and process control of optical lithography played a major role in this progress and will most likely continue to do so in the future. The beginning of the millennium has witnessed new rapid developments towards higher frequencies and new applications–such as Bluetooth which operates at 2.45 GHz. Currently, one of the main challenges for SAW filters is the need to reach frequencies up to 5 GHz, required by such emerging technologies as wireless LAN. All this development work is driven by the fact that wireless communication systems constitute a huge market for SAW components.

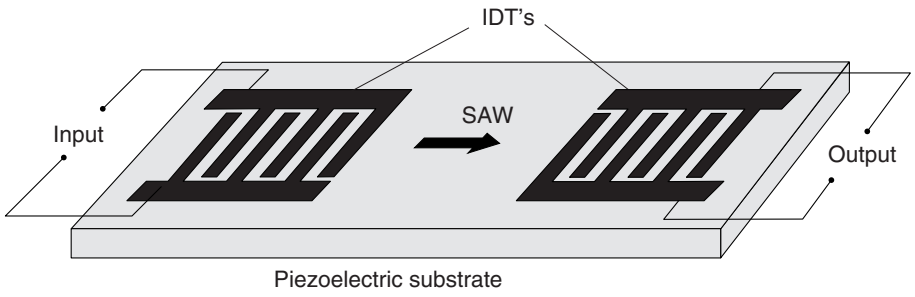

Figure 1.1: Schematic of a conventional SAW filter. It comprises a pair of IDTs, one acting as a transmitter of surface acoustic waves and the other as a receiver.

Another challenge set by wireless communication applications is the requirement of low insertion loss. The conventional SAW filter designs, mainly developed in the 1960s and 1970s, utilize the frequency dependent conversion of the electric signal into an acoustic wave with an IDT, followed by a reconversion into an electric signal with another IDT. A schematic of such a SAW filter is shown in Fig. 1.1. Due to the bidirectionality of the IDT, the conventional SAW filters have a minimum insertion loss of 6 dB. Additional losses result from electrical matching necessary for achieving, e.g., a flat passband. Total losses are typically in the range of 15-25 dB. In the communications receiver circuitry, high losses limit the usage of such SAW filters to intermediate frequency (IF) signal processing stages, operating with millivolt signal levels. Signal-to-noise limitations imposed by the high insertion loss render the conventional SAW filters unsuitable for radio frequency (RF) filtering stages involving microvolt-level inputs. Conventional SAW filters are also not applicable in the

RF transmitter circuitry where high insertion losses would lead to excessive power consumption and shortened battery time for handheld applications.

The advances made in SAW technology during the 1990s were significant. Current RF SAW filters typically feature an insertion loss within 1-2 dB. Such second-generation low-loss devices can be achieved by four main approaches developed during the past twenty years: (i) impedance element filters (IEFs) [3–7], (ii) coupled resonator filters (CRFs) [8–10], (iii) transversely coupled resonator filters (TCFs) [11–13], and (iv) interdigitated IDT structures (IIDTs) [14, 15]. Today, the RF SAW filter market is covered by IEFs and CRFs. Out of the four listed low-loss device types the first three approaches utilize SAW resonators. Thorough understanding and accurate simulation tools describing the operation of SAW resonators are required for device design–the performance of a filter is to a large extent determined by the performance of the resonators. But due to the complexity of the problem–which involves time-dependent electrical fields coupled to mechanical vibrations in an anisotropic crystal–the simulation tools inevitably have their limitations, failing to predict unexpected phenomena. In such circumstances, application of experimental probing techniques to directly measure the acoustic wave fields within the device can be instrumental.

Interferometric techniques allow the measurement of small changes of physical quantities (length, pressure, temperature, etc.) that influence the propagation properties of light. This is generally accomplished by letting two waves interfere, one undisturbed and one changed by the object. In the course of history many decisive and important experiments have utilized interferometry, such as the failed attempt by Albert A. Michelson and Edward W. Morley to measure the effect of moving ether on the velocity of light. The historic null result, as scientists call it, was the proof that ether, which at the time was commonly included in the physical interpretation of the universe, does not exist. The experiment also suggested that the speed of light plus any other added velocity was still equal only to the speed of light. To explain the results of the Michelson-Morley experiment, physicists had to search for a new and more refined foundation, something that resulted, eventually, in Albert Einstein's formulation of the special theory of relativity in 1905. Today, the speed of light is fixed to an exact numerical constant and the basic unit of length, the meter, is related to it. Typically, the calibration of length meters is achieved using carefully stabilized laser sources and optical interferometry. Interferometry also has many other applications including, e.g., optical gyroscopes which typically utilize the Sagnac interferometer. These sensitive fiber-optic gyroscopes (FOG) are utilized in inertial navigation and guidance systems on board ships, submarines, commercial jet aircrafts, carrier rockets and satellites. Also the basic research of physics may soon benefit from new results obtained with optical interferometers. Scientists at the laser interferometer gravitational wave observatory (LIGO) are attempting to detect cosmic gravitational waves with the help of 4-kilometer-long highly advanced interferometers possessing unprecedented sensitivity. Observation of gravitational waves, produced by violent events in the distant universe, such as collision of two black holes or shockwaves from

the cores of supernova explosions, could be used to verify the predictions made in 1916 by Albert Einstein in his general theory of relativity.

Owing to its ability to detect small changes, optical interferometry can be applied to studying ultrasonic vibrations, including the imaging of surface acoustic waves, a task which requires detecting minute displacements down to the nanometer scale. The main advantage of optical interferometry is the fact that the beam does not perturb the surface acoustic wave and, therefore, does not influence the operation of the SAW device. In other words, the technique is a non-contact method, which also implies that there are no fundamental restrictions on surface temperature should a need for such measurements arise. Furthermore, the point of measurement may be quickly relocated and a high spatial resolution can be obtained without reducing the sensitivity. With a suitable light source and focusing optics the measurements may be localized at a sub-micrometer level. However, it should be noted that the spatial resolution is limited by diffraction to the order of the wavelength of the light. With optical probing one can also attain a flat broadband frequency response, particularly at high frequencies, which is difficult to achieve with, e.g., piezoelectric transducers. For optical measurements the frequency limitation arises from the high-speed photodetector used. However, as photodetectors are readily available for frequencies greatly exceeding the operation range of current SAW devices, this limitation does not pose a problem for imaging SAW fields. Moreover, the vibration amplitude measurements may be directly related to the wavelength of the light and, hence, no other calibration is required. However, this typically requires the use of optical heterodyning. The main disadvantages of interferometry are that it is admittedly rather insensitive compared to the use of piezoelectric devices and that it typically requires a stable setup and careful alignment of the optical components.

The research work described in this Thesis concentrates on studying SAW resonators, more specifically resonators which utilize the leaky surface acoustic wave (LSAW). This work is carried out with an optical laser interferometer developed at the Materials Physics Laboratory specifically for the purpose of studying SAW components. A brief introduction to imaging surface acoustic waves and different imaging techniques used is given in Chapter 2 along with references to previously published results in the area of optical imaging of SAWs. Most commonly reported techniques include surface tilt detection, i.e., the knife-edge technique; surface displacement detection, i.e., interferometry; and light diffraction arising from the periodic pattern created on the surface by the surface acoustic waves, i.e., the diffraction grating technique. All of these are optical detection techniques. Other techniques and devices such as scanning acoustic force microscopy (SAFM), scanning tunneling microscopy (STM), scanning electron microscopy (SEM), the electrostatic probe and the electromagnetic acoustic transducer (EMAT) have also been applied to detection of SAWs but to a much smaller degree than optical techniques.

The scanning Michelson interferometer developed in the Materials Physics Laboratory is introduced in Chapter 3. The optical setup of the interferometer, the sample translation system, detection electronics, and control software are all briefly

explained. The achieved spatial resolution and sensitivity are also discussed. This work is reported in Paper I.

Results from the studies of LSAW resonators on lithium tantalate ($LiTaO_3$) are given in Chapter 4. Publications II, III, IV and V involve the study of an acoustic loss mechanism discovered with the scanning Michelson interferometer. This loss mechanism, resulting from leaky surface acoustic waves escaping to the busbars, can seriously degrade the performance of LSAW resonators. The results published by the author and co-authors have been widely acknowledged by other scientists and engineers working with LSAW impedance element filters. Publications VI and VII involve direct measurements of bulk acoustic wave (BAW) radiation from LSAW resonators. Such radiation into the bulk is inherent for LSAW resonators. Theoretical models and numerical simulations characterizing the phenomenon have been previously published but very few publications report direct measurements of the bulk acoustic waves radiated from LSAW resonators. The results in Publications VI and VII yield unique information on BAW radiation fields generated by a LSAW resonator on $LiTaO_3$. The conclusions and discussion are provided in Chapter 5.

2 Optical Imaging of SAW Fields

The first papers reporting detection of surface acoustic waves–or the measurement of surface vibrations–by optical means were published in the late 1960s[1] by Ippen [16], Korpel *et al.* [17], Krokstad *et al.* [18], Deferrari *et al.* [19], Mayer *et al.* [20], Auth *et al.* [21], Adler *et al.* [22], Whitman *et al.* [23], Salzmann *et al.* [24,25], Slobodnik [26], Serbyn *et al.* [27], Sizgoric *et al.* [28], Ash *et al.* [29], Soffer *et al.* [30], Lean *et al.* [31–33] and Richardson *et al.* [34]. In these papers the three main optical techniques for detection of surface acoustic waves are presented: various implementations of the diffraction grating technique [16–18,20,21,24–26,30–33], the knife-edge technique [22] and the detection of ultrasonic vibrations using optical interferometry [19,23,27–29]. A non-optical method, i.e., the electrostatic probing technique was also introduced [34]. During the 1970s a wealth of papers continued to report on optical detection methods of SAWs and on various parameters determined from the experiments [35–87]. The diffraction grating technique was widely applied during the end of the 1960s and throughout the 1970s, while the knife-edge technique and interferometry, both of which allow high-resolution phase-sensitive detection, have gained popularity during the 1980s and 1990s.

Many excellent review articles and book chapters on the detection of SAWs have been published [88–98]. They provide the reader with a thorough introduction on the various techniques and the key results obtained. However, since many of the non-optical methods were not applied or invented at the time of publication of these reviews, they discuss mainly or solely the optical methods. This is in line with the fact that the majority of the results obtained via direct probing of SAWs have been achieved by applying optical imaging techniques. The usefulness of these review articles cannot be overemphasized if one is interested in the field of SAW imaging.

Direct measurement of the ultrasonic vibration on the substrate surface can be used for a variety of purposes which range, in one extreme, from fundamental work on studying acoustic-wave physics to simultaneously measuring and tuning an operative SAW component in the other extreme. Practically all the important wave propagation parameters such as velocity [21, 29, 30, 35, 41, 43, 53, 72, 73, 79, 99–128], attenuation [17,24,26,31–33,37,38,41,48,49,51,53,76,100,101,107,110–112,117,121,124,129–135], beam-steering [33, 36, 38, 48, 63, 123, 131], beam focusing [22, 63, 136–145], diffraction [22,30,33,38,41,44,48,52,57,62,70,76,100,101,103,111,113,118,126,146–150], refraction [103, 150], scattering [45], aberration [151], transduction [36, 61, 152, 153], reflection [22, 33, 51, 53, 72, 74, 81, 86, 105, 112, 152–156], transmission [33, 51, 86], waveguiding effects [29,50,66,146,154,157,158], and the generation of harmonics [31–33,37,42,43,49,53,59,64,65,67,76,77,133–135,159,160] can be obtained by directly measuring the

[1] Here the term 'first papers' refers to the time after the invention of the laser and the IDT. Earlier work on optical detection of ultrasonic waves, dating back to the 1920s, does exist. See, e.g., the review papers of White [89], Stegeman [92] and Royer [98] for details.

acoustic vibrations. Also the value of the piezoelectric coupling coefficient (K^2) can be determined [107,117]. In addition, the generation and build-up of surface acoustic waves within, and emitted by, IDT structures [54,55,69,152,161–166] can be directly measured, as well as the the standing wave ratio [53, 78, 80, 84]. The operation of multistrip couplers and beam compressors can be evaluated [62, 81, 161]. Radiation into BAWs and BAW reflections from substrate interfaces may be investigated [18,39, 46,47,56,59–61,68,71,72,75,82,83,85–87,112,125,153,167,168]. Also the bulk particle motion fields of SAWs have been measured [169]. Identification of different wave types, such as the Rayleigh SAW, leaky SAW, surface skimming bulk wave (SSBW), etc., is possible via visualization and analysis of surface-wave fields [123,126,153,170]. For longitudinally and transversely coupled SAW resonator filters (CRF and TCF, respectively), different longitudinal and transversal modes can be directly verified [155, 171–176]. Also operation of reflective array compressors (RACs) and slanted array compressors (SACs) have been studied using optical probing [103, 112, 130, 150, 164, 177, 178]. The surface acoustic wave dispersion relation for various wave types can also be directly derived by probing suitable test structures [42, 110, 127, 170, 175]. In addition, undesired acoustic losses occurring in SAW resonators due to waveguide failure [179–182, II–V] or synchronous radiation to Rayleigh-wave modes can be studied [183].

It should be emphasized that some of the above mentioned parameters or phenomena are either impossible or extremely difficult to determine via mere electrical measurements. Thus, for studying parameters such as diffraction [22, 30, 33, 38, 41, 44, 48, 52, 57, 62, 70, 76, 100, 101, 103, 111, 113, 118, 126, 146–150], the generation and build-up of surface acoustic waves within IDT structures [54,55,69,152,161,164,165], mode symmetry distortions due to anisotropy [173] or the second-order leakage mechanisms [179–182, II–V], direct probing of the acoustic vibrations is the only viable technique. It should also be noted that the list of parameters given above is by no means comprehensive. It is merely an attempt to show that a vast number of applications for SAW visualization exists. As a slight overstatement one might argue that any required parameter involved with designing SAW applications can be derived directly from the measurements, provided that one is able to determine the acoustic wave amplitude and/or phase either as a function of frequency or location, or as a function of both, and with sufficient accuracy. However, it should be noted that fulfilling the above conditions in practice can present a great challenge as well as require very sophisticated measuring equipment.

The most severe demand for any given visualization technique is the high sensitivity required to detect surface vibrations associated to surface acoustic waves. Typical surface displacements in SAW components usually range from 10^{-11} m to 10^{-8} m, i.e., from 0.01 nm up to 10 nm. However, if weak second-order effects are to be studied, amplitudes as low as 0.001 nm may need to be detected. This requirement can be compared to the typical thermal vibration amplitudes of aluminium atoms on the surface of an aluminium layer in room temperature: $\sim$0.01 nm [184].

Further challenges arise if the acoustic wave has no out-of-plane oscillation compo-

nents. This condition applies, e.g., to surface transverse waves (STWs), high velocity pseudo surface acoustic waves (HVPSAWs), Bleustein-Gulyaev waves (BGWs), Love waves, and surface skimming bulk waves (SSBWs). In these cases, detection methods which measure the out-of-plane surface shift or the tilt of the surface are not applicable.

If individual wavefronts are to be separated, requirements for the spatial resolution (i.e., the area of the active probe tip, beam or the wavelength of the sampling wavefield) increase linearly with increasing SAW frequency, provided that the wave velocity remains constant. For low-frequency components operating in the 10 MHz to 100 MHz regime, assuming the SAW velocity to be in the range 3000. . .5000 m/s, typical SAW wavelengths vary from 0.5 mm down to 0.03 mm (30 μm). Such resolutions can easily be obtained via optical techniques (or even with physical probes). However, for SAW frequencies at 1 GHz the wavelength is approximately 4 μm. Since the period of a standing wave field is only half of this (2 μm), very stringent demands are set for the spatial resolution of the probe. For optical methods utilizing He-Ne lasers of wavelength $\lambda\sim$0.63 μm, the smallest achievable (realizable diffraction-limited) spotsize is below 1 μm. With the help of short-wavelength UV-lasers, spotsizes below 0.5 μm can be achieved. Hence, optical methods are well suited up to 1 GHz and above but cannot provide sub-wavelength spatial resolution at frequencies beyond 2 GHz. However, it should be noted that in some cases the sub-wavelength resolution is not required. The parameters sought for can be successfully determined at a lower spatial resolution [164, 165, 185]. Should sub-wavelength resolution above 2 GHz be required, it can be achieved for example with the help of atomic force microscopes.

The typical probed surface in passive SAW components is divided into areas of polished crystal and deposited aluminium. The piezoelectric crystal material is usually lithium tantalate ($LiTaO_3$), lithium niobate ($LiNbO_3$) or quartz (SiO_2). All of these crystals are optically transparent and qualify as electrical isolators. In strong contradiction, the aluminium used for IDTs, reflector gratings, busbars, signal leads and bond-wire pads is optically opaque, strongly reflective and has good conductivity. Special SAW components, e.g., high-frequency components, high-power filters or chemical SAW sensors, may also feature various other materials such as gold, copper, nickel, mixed metals, diamond, ZnO, AlN, PZT and chemically active thin films. However, the overwhelming majority of SAW components utilize one of the crystal materials listed above along with aluminium. The differences in the optical properties of the crystal material and the areas coated with aluminium often result in different sensitivities for the probe, depending on whether the measurement takes place on top of the crystal surface or on top of the areas with deposited aluminium. For accurate parameter extraction, the measurements can be limited to areas with uniform surface properties, or, normalization techniques can be applied. Some probing techniques are only effective either for crystal surfaces [34, 175, 181] or for metallized surfaces [186, 187].

If the acoustic field in a production component, instead of that in a custom-designed test sample, needs to be imaged, some additional difficulties may arise due

to the package and bond wires included in the assembly. The line of sight to the crystal surface may be obstructed by the bond wires. It may also be difficult to place the optical system or the probe tip assembly physically close enough to the surface of the chip due to the edges of the package and/or the bond wires. However, with suitable optical components successful probing can be achieved even from packaged samples, provided that the package lid has been removed [I].

3 Scanning Michelson Interferometer

3.1 Optical Setup

The optical setup of the imaging system utilized in this work is a homodyne Michelson interferometer. The setup features a good sensitivity and a simple optical construction which enables straightforward beam control and focusing onto the sample.

Figure 3.1 shows a schematic of the Michelson interferometer. Light from the laser is guided to the polarizing beamsplitter which divides the beam into the measuring beam and the reference beam. The reference beam is reflected from the mirror and it returns to the beamsplitter. On first pass through the $\lambda/4$ plate, the reference beam becomes circularly polarized, is reflected from the mirror and traverses the $\lambda/4$ plate in the reverse direction. The polarization of the returning beam has now turned 90° from the original direction and it passes through the beamsplitter directly onto the analyzer. The measuring beam is focused onto the sample surface, it becomes phase modulated by the surface acoustic vibrations, and is reflected back to the beamsplitter. Again, a $\lambda/4$ plate is used to rotate the polarization by 90°. Thus, the reflected measuring beam is guided through the beamsplitter onto the analyzer. An additional glass plate is used to direct a small portion of the beam onto a photodetector. The signal from this detector is used to record the light intensity reflected from the sample.

An analyzer projects the polarizations of the measuring and the reference beam onto the same plane and the two signals interfere on a high-speed detector. The first two Bessel terms of the frequency-modulation spectrum at the detector are given by

$$P \sim E^2 + E'^2 + 2EE'[J_0(C)\cos(\phi) - 2J_1(C)\sin\omega_{SAW}t\sin\phi]. \tag{3.1}$$

Here the electric components of the fields for the measurement and reference beams are denoted by E and E', respectively. The last term oscillating at the frequency ω_{SAW} is proportional to the surface vibration. The Bessel function of the first kind of order one, $J_1(C)$, is linear to a good accuracy for small arguments with values less than 0.6. A theoretical limit for linear detection may be estimated from $C = 4\pi A/\lambda \leq 0.6$, where λ is the wavelength of the laser source (632.8 nm). This gives a value of 30 nm for the maximum vibration amplitude A that can be measured with a good accuracy. Typical values for the surface acoustic amplitudes are on the order of a few nanometers; hence, the condition for linear detection is valid.

It should be noted that the amplitude is modulated by the $\sin\phi$ term, where ϕ is the phase difference between the reference beam and the measuring beam. For optimal efficiency, it should be set equal to $\pi/2 + n\pi$. It can be shifted by adjusting the optical path difference, that is, by moving the mirror or the sample.

The light source is a linearly polarized TEM_{00}-mode He-Ne laser. The laser model is Uniphase 1135P (λ = 632.8 nm, P_{out}=10 mW). The microscope objective is a Nikon 354248 CF N Plan 40 x ELWD, which has a numerical aperture of 0.55 and

a working distance of 5.08-6.84 mm. The high-speed photodetector is a Newport 818-BB-21, which according to the manufacturer has a bandwidth of 400 MHz. However, measurements have shown the bandwidth to extend well beyond 2 GHz when the impedance matching between the detector and the subsequent RF-amplifier is carefully selected. Most of the optical components, mirrors, $\lambda/4$-plates and collimating lenses are from Newport. The optical table is a Performance Plus model from Melles-Griot.

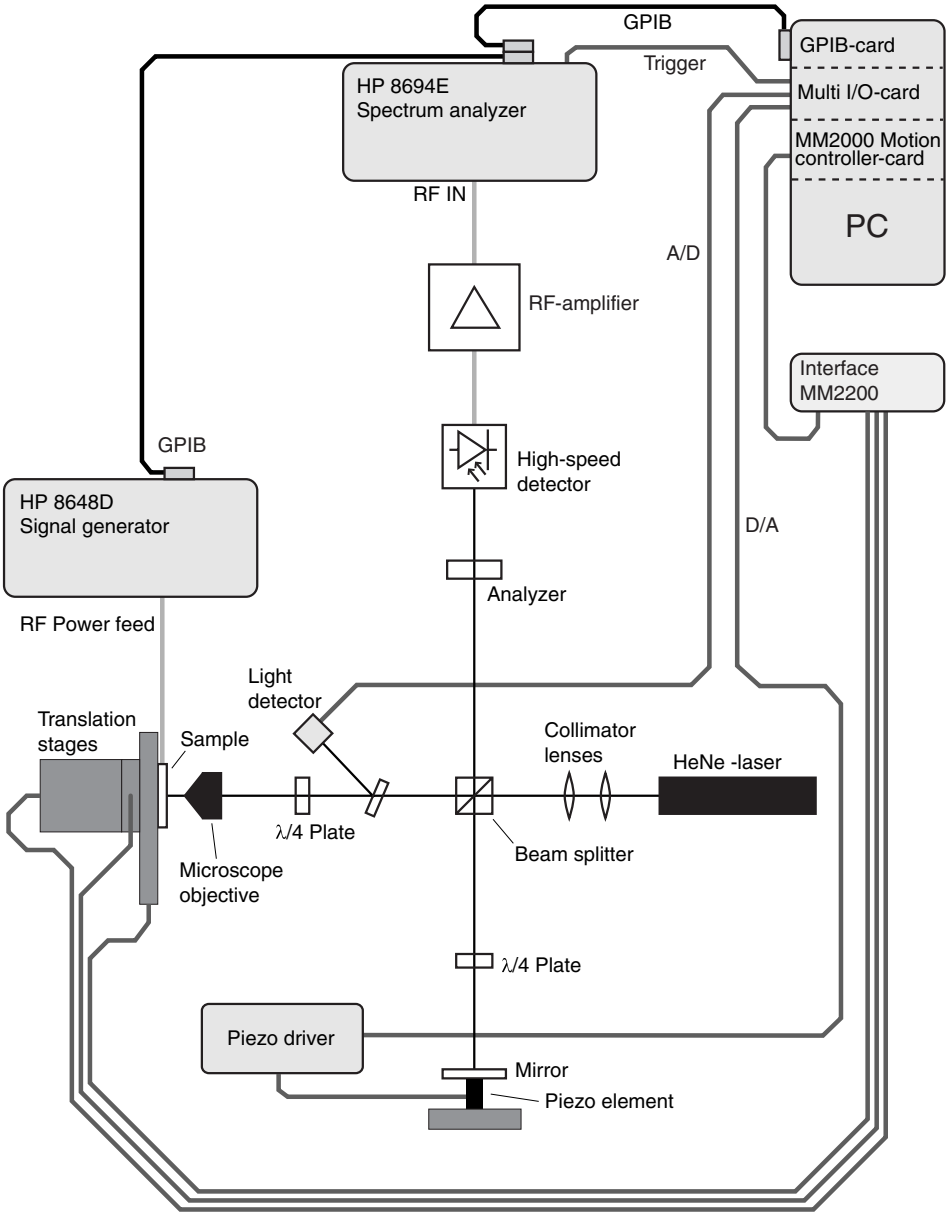

Figure 3.1: Schematic of the Michelson interferometer. Optical setup, sample translation stages, RF electronics, signal generator, spectrum analyzer and the piezo driver unit are shown.

3.1.1 Spatial Resolution

The spatial resolution is determined by the area of the focused laser beam. The initial laser beam is the transversal mode TEM_{00}, and it features a Gaussian intensity profile. When such a beam is focused, the smallest achievable beam diameter, defined as the $1/e^2$ width, is [188, p. 419 and p. 187]:

$$\delta = \frac{4\lambda f}{\pi d} = \frac{2\lambda}{\pi NA} \quad , \tag{3.2}$$

where d is the beam diameter before the focusing lens, f is the focal length of the lens and λ is the wavelength of the laser. The quantity NA is the numerical aperture. It characterizes the focusing capabilities of the lens, provided that the incoming beam fills the aperture of the focusing lens.

By increasing the width of the incoming beam, it is possible to achieve a smaller focused spotsize. In practice, this is limited by the aperture of the lens. A shorter focal length also results in a smaller spotsize but leads to a smaller depth of focus which complicates maintaining focus. The numerical aperture contains information on both of these lens properties and can be used to calculate the smallest achievable spotsize. For the Nikon CF N Plan 40x, the NA is 0.55. Applying Eq. (3.2) yields approximately 0.73 μm for the smallest possible spot diameter for the laser source used, provided that the incoming beam fills the aperture of the objective. The xy-translation stages, Newport model MFN25CC, applied for moving the sample have a minimum step of 0.055 μm. However, this value merely defines the minimum incremental step at which the sample can be shifted. It does not give the spatial resolution of the setup, which is determined solely by the spotsize, calculated here to be 0.73 μm.

It should also be noted that the spotsize sets a possible upper limit to the frequency range of the laser probe. The diameter of the measuring beam must be less than half the wavelength of the surface acoustic wave. Thus the surface acoustic wavelength must be longer than 1.5 μm, yielding an upper theoretical limit of 2.7 GHz. Here the velocity of the surface acoustic wave is assumed to be approximately 4000 m/s. However, in practice the measuring electronics, especially the bandwidth of the high-speed photodetector used, is much lower than the 2.7 GHz estimated as the spotsize-limited detection bandwidth.

3.1.2 Sensitivity

For achieving maximal amplitude resolution, several conditions must be fulfilled. The phase difference between the measuring and the reference beam must be $\pi/2 + n\pi$. Unless the beams are accurately aligned, slight phase differences will occur across the area of the detector where the beams interfere, and the measured signal will weaken [97, pp. 87-89]. Poor collimation of the beams can also result in similar phase differences and loss of sensitivity.

The reflectivity of the sample surface should be high. If the surface possesses a low reflectivity, the reflected measuring beam will have a low intensity in comparison to the reference beam. This imbalance will decrease the interference signal.

Although the optical conditions are critical for the sensitivity of the setup, it is the electronics and especially the photodetector–along with the preamplifier–which set the lower limit for the detectable surface vibration. Poor noise characteristics of the photodetector and the amplifier will result in inferior amplitude resolution even if the optical components were selected and positioned with the greatest care. Taking the above factors into consideration the minimum shot-noise-limited detectable surface vibration, or noise-equivalent displacement for a diffusing surface is given by Scruby and Drain [97, p. 96] as

$$A_{min} = \frac{1}{4}\delta\Big(\frac{h\nu\Delta f}{\eta P_{out}}\Big)^{1/2} \quad , \tag{3.3}$$

where δ is the focused spotsize, h is the Planck constant, Δf is the selected detection bandwidth, ν is the light frequency, η is the quantum efficiency of the detector and P_{out} is the laser power.

According to the manufacturer, the quantum efficiency of the Newport 818-BB-21 detector at the wavelength 632.8 nm is 0.55. Calculating the minimum resolution for a 0.7 μm spotsize we obtain a value of $0.3 \cdot 10^{-4}$Å$/\sqrt{\text{Hz}}$ for the calculated sensitivity. In order to determine the sensitivity experimentally, a piezoelectric element equipped with a reflecting mirror surface was used to replace the sample. To achieve the calibration of the interferometer signal and the surface vibration amplitude of the sample, the measured signals at the drive frequency (400 kHz) and at the second-harmonic and third-harmonic frequencies were recorded at different drive levels of the piezoelectric element and fitted to the values of the corresponding Bessel functions given by the modulation theory. A minimum detectable surface displacement of $1.1 \pm 0.2 \cdot 10^{-2}$Å for a 10 kHz detection bandwidth was obtained, resulting in a sensitivity of $1.1 \pm 0.2 \cdot 10^{-4}$Å$/\sqrt{\text{Hz}}$ for the probe. The higher detection limit, compared with the calculated value, is due to the light intensity and coherence losses at the nonideal optical surfaces and the added noise resulting from the amplification of the detector signal.

3.2 Accessories

In addition to the optical components and the photodetectors, a number of other instruments are required for creating a measurement system capable of producing areal scans of the surface acoustic wave field. The computer, RF electronics and the translation stages needed to supplement the interferometer into a fully operative system are shown in Figure 3.1.

3.2.1 Detection Electronics

The RF electronics of the setup include a low-noise amplifier, spectrum analyzer and a signal generator. Two optional amplifiers may be used. For the low-frequency samples, operating below 500 MHz, a Mini-Circuits low-noise broadband model ZFL-500LN is employed. It possesses a gain of 24 dB, a noise figure of 2.9 dB and its

bandwidth is 0.1–500 MHz. For high-frequency samples, a Mini-Circuits low-noise model ZFL-1000LN is applied. It features a gain of 20 dB, the noise figure is 2.9 dB, and its bandwidth is 0.1–1000 MHz. Both amplifiers act as high-pass filters and, thus, no DC signal is passed on to the spectrum analyzer. The spectrum analyzer is a Hewlett-Packard model 8594E. It has a bandwidth of 9 kHz – 2.9 GHz and can be fully controlled via the general-purpose interface bus (GPIB). It is also capable of operating in a zero-span mode. This enables one to measure the amplitude of a selected frequency as a function of time. The receiver bandwidth may be selected in the range from 1 kHz to 3 MHz. The signal generator used as the RF power source is a Hewlett-Packard model 8648D. It has a bandwidth of 9 kHz – 4 GHz and maximum output power of 21 dBm. It can also be fully controlled via the GPIB.

When the correct signal from a measuring point is to be achieved, two separate phenomena must be considered. First, the sample surface must be at the focus of the objective. Second, the phase difference between the measuring and the reference beams must equal $\pi/2 + n\pi$. Tuning the interferometer at each point is achieved by applying a fast scheme which locates the quadrature points of the signal. The spectrum analyzer is set to zero-span mode, where it acts as a tuned receiver and records the amplitude of the tuned frequency as a function of time. Since the reference mirror is simultaneously moved with the piezo element, the response of the interferometer is obtained as function of the path difference over a few optical wavelengths. From this response, four maxima are located and averaged to yield the SAW amplitude. The receiver bandwidth of the spectrum analyzer is set to 3 kHz. A narrower receiver bandwidth can be used to increase the sensitivity but this is limited by the spectrum analyzer. The applied scheme serves to eliminate the need for stabilization circuits and provides a high tolerance against external low-frequency vibrations since a narrow receiver band is applied and the signal maxima are always detected. The sweep can be performed in less than 50 ms, thus enabling measuring speeds above 70 000 points/hour. However, the translation stages limit the highest achieved scanning speed to 50 000 points/hour.

3.2.2 RF Shielding

Radio frequency (RF) shielding is required to prevent the direct leakage of the RF signal from the sample to the detector. This radio-frequency interference (RFI) distorts the results since it produces a constant amplitude at the spectrum analyzer. By attenuating the leakage to a level below the measurement noise level it proves possible to remove this distortion from the results. Leakage can either be due to a direct radiation from the sample, or it can be caused by conduction through electronics. Direct conduction can be isolated by keeping the RF signal generator and the detection electronics electrically separated. Yet, in the present system this is not possible since the spectrum analyzer and the signal generator must share a common GPIB data cable. Fortunately, the GPIB ports of these devices are efficiently isolated from the RF electronics. Therefore, direct conduction does not pose a problem. However, radiation from the RF power feed cable, the jig and the sample creates

serious problems. This is due to the high frequency of the signal, which varies from 100 MHz up to 1 GHz, depending on the sample under study. Since above 30 MHz the leaked signal is usually radiated, it is clear that the possible leakage problems are to be attributed to the radiation leakage. Such leakage can be suppressed either by shielding the detection electronics from the radiation or by preventing radiation at the source, i.e., the RF power feed cable, the jig assembly, and the SAW sample. With the interferometer, both methods have been implemented.

To shield the detecting electronics, the high-speed photodetector is placed in a solid steel case equipped with a removable lid. A hole with a small diameter allows the laser beam to reach to the detector. The electrical connection to the box is completed with carefully grounded connectors and, in addition, the cables running from the detector to the RF amplifier and from the amplifier to the spectrum analyzer possess high screening efficiency of 120 dB for frequencies ranging from 100 MHz to 1 GHz. In order to eliminate RF radiation at the source, the SAW sample, translation stages and the jig assembly are enclosed into an aluminum case with a detachable lid and side walls. Again, considerable effort has been taken to ensure proper connections from and into the shielding case. The RF power is fed through a grounded connector and the voltage and controlling signals operating the translation stages are connected via RF-filtered multipin connectors providing more than 40 dB of RFI attenuation at 1 GHz. This prevents possible RF leakage induced into the data cables within the case from escaping the enclosure.

With all the above arrangements, a typical leakage signal measured at the spectrum analyzer is -120 dBm when a 1 GHz SAW sample is being driven with $+20$ dBm RF power. Since the noise level of the detector signal is approximately -108 dBm, the RF leakage is well below the noise limit and does not distort the measurement. For lower frequencies, in the range of $100 - 200$ MHz, the leakage signal is already unmeasurably small. Apart from preventing the direct leakage of the RF signal from the sample into the detector, the RF shielding also serves to effectively prevent external sources, such as radio or mobile phone transmissions, from interfering with the measurements.

3.2.3 Control Software

The tasks of controlling the high-precision translation stages, multi I/O card, GPIB card, signal generator and the spectrum analyzer are handled by the control software. Although most of the functions performed by the software could be accomplished with a commercially available software package such as Labview, there are some procedures where optimized code is necessary. In particular, the mirror sweeping sequence requires the possibility to tune the code freely in order to achieve the maximum speed. Therefore, the control software has been fully programmed in house. The programming, including the graphical user interface, was carried out with Visual Basic. The user interface provides the necessary flexibility needed in configuring, tuning and operating the measuring devices and in selecting the scanning parameters. The user is able to simultaneously access the translation stages, the signal generator, the spectrum analyzer, and the scanning parameters from a single screen.

4 Acoustic Losses in Leaky SAW Resonators

4.1 Leakage to Busbars - "The Banana"

Leaky surface-acoustic wave (LSAW) devices operating at radio frequencies are widely employed in modern telecommunication systems. Electrical measurements of LSAW resonators on rotated Y-cut lithium tantalate ($LiTaO_3$) substrate [189] typically feature losses not predicted by phenomenological models which assume an infinite aperture [194], see Fig. 4.1. The same limitation often applies to other fast analysis models used for LSAW, such as coupling-of-modes (COM) models [190–193]. Hence, possible 2D effects are typically not included in the simulations.

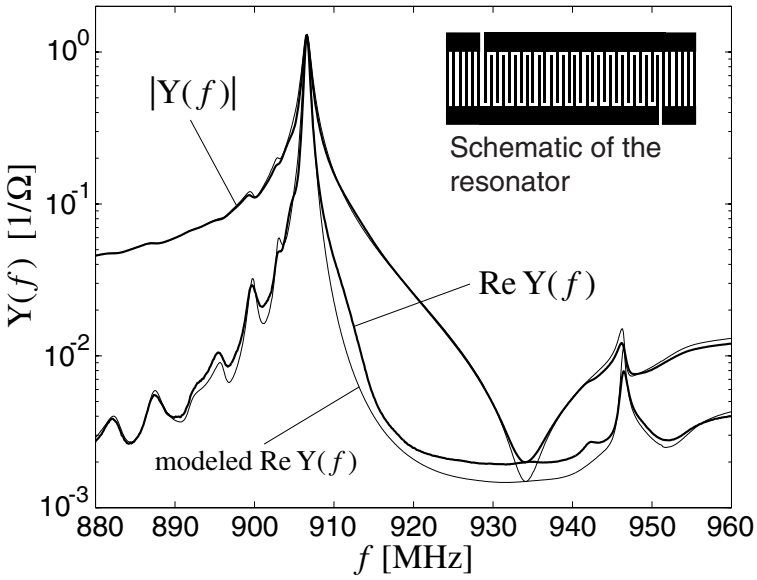

Figure 4.1: Measured admittance and conductance of a synchronous resonator as a function of frequency. Also shown are the results from a phenomenological model [194]: the modeled conductances, i.e., losses, are too low.

Early laser-interferometric measurement of a 947.5 MHz GSM Rx SAW filter on 36° $LiTaO_3$ supporting a leaky SAW mode showed evidence of surface acoustic waves escaping from the parallel resonators of the ladder-type impedance element filter [195]. This discovery inspired further measurements even though at the time the connection between the unexplained electrical losses and the observed leakage was not recognized.

4.1.1 Interferometric Measurements

Leakage to busbars similar to that published in [195] was observed in the series resonator of a ladder-type impedance element duplexer intended for the ISM band realized on 36° YX-cut $LiTaO_3$. These results were reported in Paper II. The banana-shaped form of the leakage evident in Fig. 1 of Paper II resulted in the nickname "banana" for the discovered leakage effect.[1] Soon after the escaping acoustic beams were identified as leaky surface acoustic waves and their behaviour was qualitatively explained through the crystalline anisotropy of the lithium tantalate substrate [III]. Further evidence of the leakage was observed also in parallel resonators of a duplexer [IV]. This observation helped to explain the mismatch in the passband part of the response curves between the improved coupling-of-modes (COM) model and the circuit simulation [IV]. The circuit simulation in Paper IV was extensive, taking into account the inductive, resistive and capacitive package parasitic effects. Outside the passband, the levels of suppression were correctly predicted by the improved COM model and the circuit simulation. This further emphasized the frequency dependence of the discovered leakage effect.

Selected laser-interferometric scans, measured from a single test resonator encompassing 120 electrode pairs in the IDT and 50 electrodes in each reflector, are illustrated in Fig. 4.2. The resonator is aligned with the crystal X-axis. The scanning steps of the translation stages were chosen as 0.495 μm along the length of the resonator and 0.99 μm in the transverse direction. The number of measurement points in the longitudinal and transverse direction were 1900 and 230, respectively. It should be noted that the interferometer only detects the time-averaged value of the shear vertical component and that the displacements on the metallized and free crystal surfaces are not in scale. This is the combined effect of two mechanisms. First, the interferometer response drops on top of the crystal surface as the reflected beam intensity drops significantly. As discussed in Chapter 3, this leads to a reduced signal level. Second, on the metallized surface, the ratio of the shear vertical component of the particle displacement–detected by the interferometer–to the dominating transversal component is small for the LSAW, and, on crystal surface, it reduces further [153,197].

Independent experimental evidence of the leakage mechanism was provided by Miyamoto, Wakana, and Ito from Fujitsu Laboratories. They published results both in 2002 [181] and 2003 [182]. Their use of polarization detection through the crystal enabled the study of the dominating shear transversal component. Hence, in addition to independently confirming the existence of the busbar leakage, the work of Miyamoto and his colleagues also proved correct the predictions given in Papers III and V regarding the symmetrical nature of the shear transversal component of the leakage.

[1] This nickname should not be confused with the piezoelectric crystal $Ba_2NaNb_5O_{15}$ which has also been referred to as "banana" [196, p. 254]

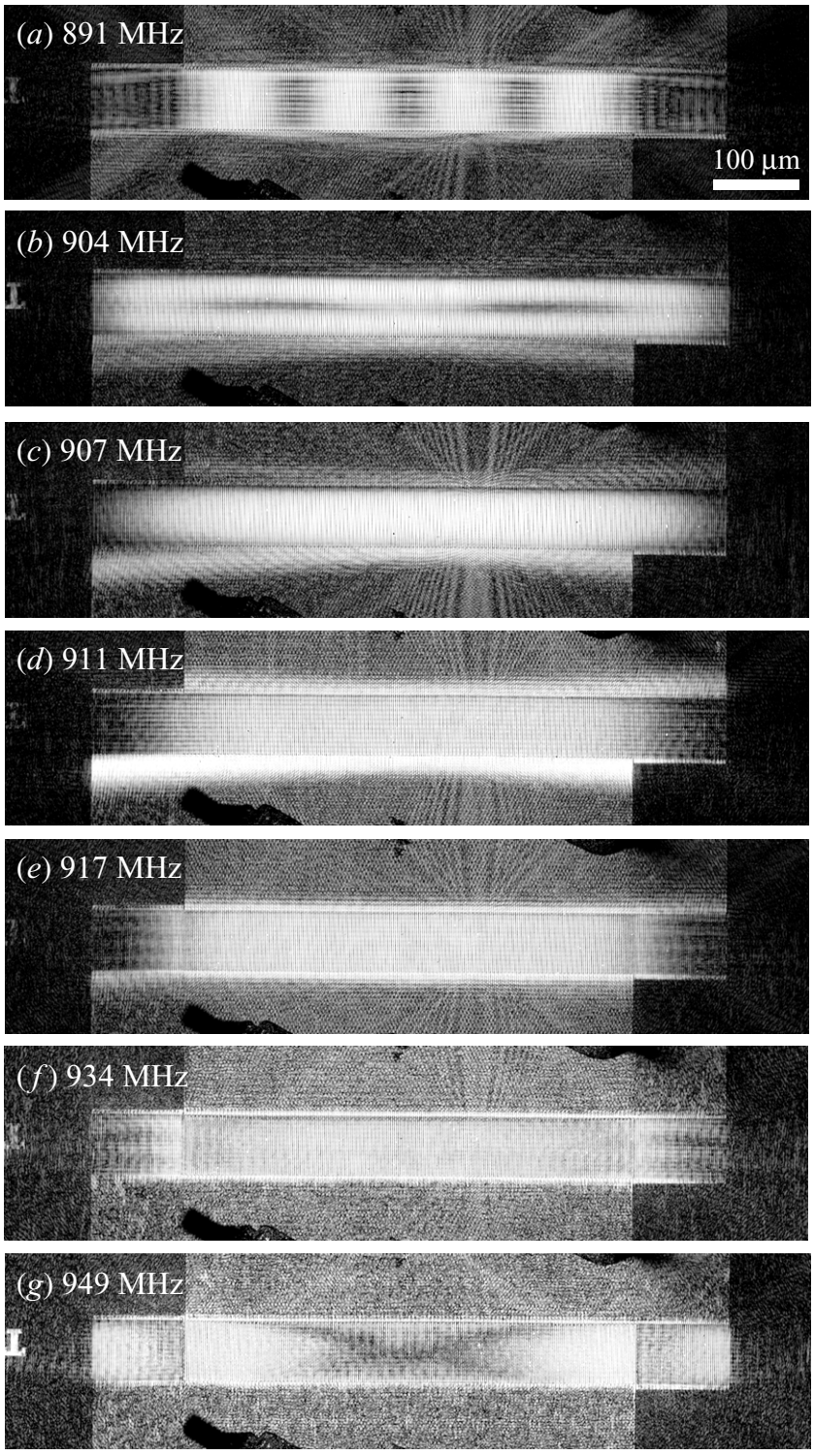

Figure 4.2: Experimental shear vertical displacement profiles measured with a laser probe, featuring LSAW radiation to the busbars in a test resonator on 36°YX-cut $LiTaO_3$. Below the resonance frequency (a, b) the radiation is weak, but strong radiation occurs slightly above the resonance (c, d). Towards a quenching frequency of about 917 MHz the radiation diminishes (e) and virtually disappears (f, g). The displacements on the metallized and free crystal surfaces are not in scale.

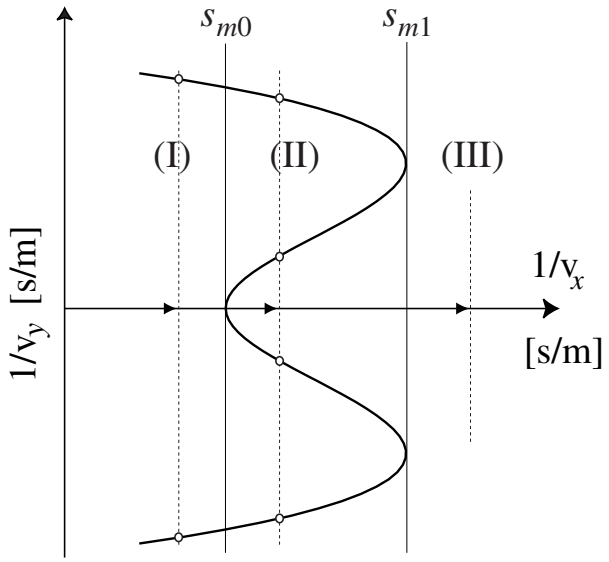

Figure 4.3: Schematic LSAW slowness curve. Depending on the slowness along x, two (weak radiation regime, I) four (strong radiation regime, II) or zero (radiation-free regime, III) LSAW modes may exist.

4.1.2 Theoretical Analysis

The strong frequency dependence of the LSAW radiation to the busbars may be qualitatively understood on the basis of the curvature of the LSAW slowness curves. As illustrated in Fig. 4.3, these may be characterized by two thresholds: the slowness for LSAW propagating along the X-axis of the crystal, s_{m0}, and the maximum x-component of the slowness, s_{m1}. Both slowness thresholds are functions of the frequency-thickness product fh, where h is the metallization thickness.

Because the busbars are of uniform metal, synchronous radiation of the LSAWs into the busbars is possible if the metallized crystal surface supports propagating eigenmodes with the same x slowness. Comparing the standing-field slowness s_x with the threshold slownesses s_{m0} and s_{m1}, three radiation regimes are identified, separated by solid lines in Fig. 4.3.

1. Regime of weak radiation (I). For $|s_x| < s_{m0}$, the metallized surface supports a pair of LSAW eigenmodes with transverse slownesses $|s_y|$. Consequently, synchronous busbar radiation is allowed but, because the corresponding transverse wavenumbers are fairly large, the coupling to the field in the resonator is weak.

2. Regime of strong radiation (II). For $s_{m0} < |s_x| < s_{m1}$, the metallized surface features two pairs of LSAW eigenmodes which merge into one pair as $|s_x| \to s_{m1}$. For $|s_x| \sim s_{m0}$, the transverse slownesses are very small for one of the pairs, and acoustic energy propagates almost parallel to the crystal X-axis. Hence, the coupling to the standing wave field in the active region may be considerable, and pronounced LSAW radiation to the busbars is expected. The strength of the excitation depends on the structure.

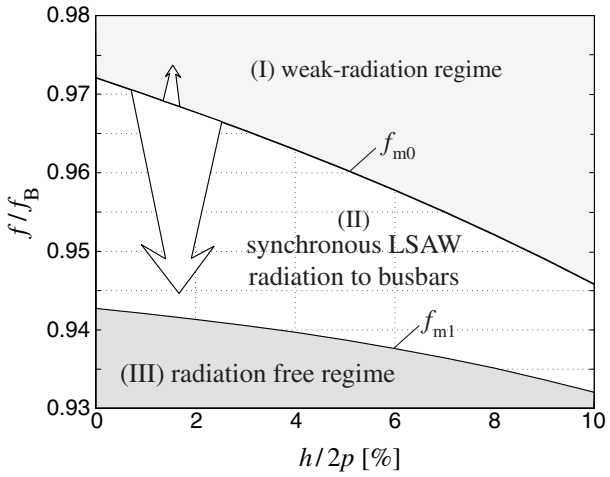

Figure 4.4: Estimated relative stopband frequencies f/f_B prone to synchronous LSAW busbar radiation on 42° $LiTaO_3$, as a function of the relative metal thickness $h/2p$. Here, f_B denotes the bulk-wave threshold frequency $v_B/2p$, with v_B=4226.5 m/s.

3. Radiation-free regime (III). For $|s_x| > s_{m1}$, there are no LSAW eigenmodes on a metallized surface. Synchronous busbar radiation is prohibited, but weak non-synchronous radiation may occur.

It should be noted that the relative threshold frequencies obtained only depend on the relative film thickness $h/2p$ in the busbars. Here, p is the center-to-center distance of adjacent electrodes. The relative threshold frequencies are independent of, for example, the shape and the width of the electrodes.

The threshold frequencies are shown in Fig 4.4 for the 42°-cut $LiTaO_3$. For the metallization thickness ($h/2p = 5.6\%$) and the pitch of the test resonator ($p = 2.214$ μm) an upper threshold frequency of about 916.7 MHz is predicted. This agrees well with both the laser-interferometric images, see Fig 4.2, and the parasitic conductance observed in Fig 4.1. The former comparison also confirms that the radiation in the regime of weak radiation is indeed faint as predicted by theory.

Due to the anisotropy of the substrate crystal the detected radiation is spatially asymmetric. Although the LSAW slowness curves are symmetric about the crystal X-axis, the polarization is not, see Fig. 4.5. The asymmetry of polarization is particularly strong for the shear vertical component U_3 detected by the interferometer, explaining the observed asymmetry of the leakage.

In addition to the qualitative analysis, a phenomenological simulation was carried out to estimate the losses caused by the LSAW busbar radiation [V]. The outcome of the simulation is that the busbar radiation well explains the experimentally observed increase in the conductance close to the resonance frequency, see Fig. 4.1.

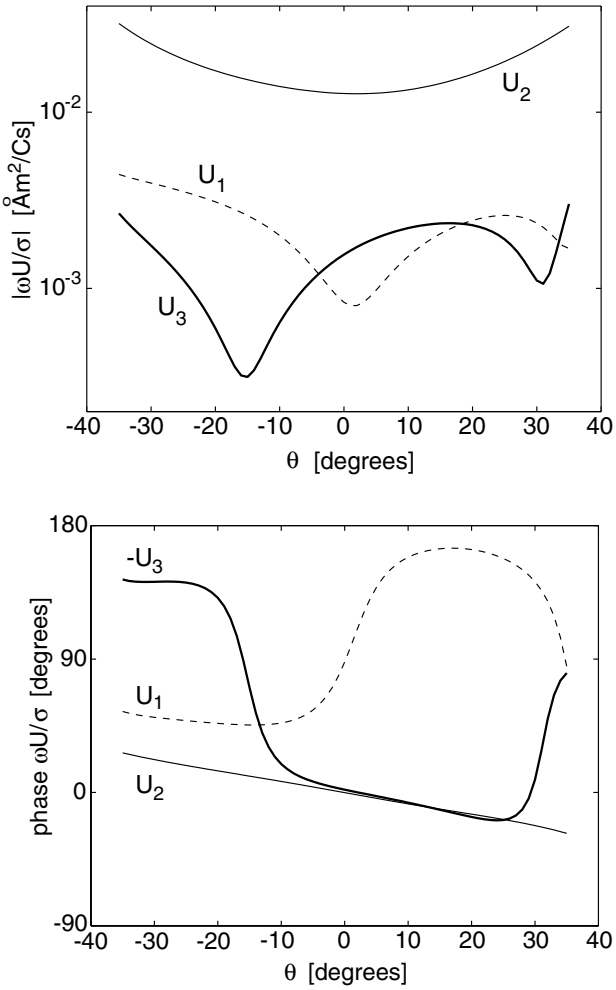

Figure 4.5: Computed polarization for LSAWs propagating on a metallized $LiTaO_3$ surface at an angle θ with respect to the crystal X-axis: (a) the relative magnitude and (b) the relative phase of components of mechanical displacement, normalized to the angular frequency $\omega = 2\pi f$ and the charge density σ. The displacement components are; U_1 longitudinal, U_2 shear horizontal and U_3 shear vertical. Out of these, the shear horizontal displacement is dominant while the shear vertical component is detected by the interferometer.

4.2 Bulk Acoustic Wave Radiation

The earlier work related to bulk acoustic wave radiation in surface acoustic wave devices is extensive. The first experimental results date back to 1967 [18], and several studies were made in the 70s [39, 46, 47, 56, 59–61, 68, 71, 72, 75, 82, 83, 85–87] while more recent research papers, involving direct detection of BAWs, appear to be few in number and involve very few groups [112, 125, 153, 167, 168]. The measurements of BAW fields reported by Chiba and Togami are particularly impressive: they provide direct information on the propagation of BAWs inside $LiTaO_3$ and $LiNbO_3$ and on BAW reflections from crystal interfaces [75,83,85]. Goruk *et al.* have also obtained impressive results by using various optical detection techniques [72,82,86,87]. However, the only reported experimental measurement of BAW radiation in LSAW resonators appears to be that of Jen and Hartmann [153]. They applied a knife-edge detection technique and Fourier analysis and succeeded in demonstrating the existence of slow shear bulk acoustic waves (SSBAW) reflected from the crystal bottom interface and arriving on the top side of the substrate. Prior to this, Hartmann and Plessky had reported electrical measurements which indirectly indicated the existence of SSBAW propagation path in LSAW test samples [198].

4.2.1 Interferometric Measurements

In order to study the BAW radiation from LSAW resonators, we applied our interferometer to measure a specially constructed sample, see Fig 4.6, which enabled laser probing directly from the backside of the substrate [VI]. The measured profiles are shown in the series of scans in Fig 4.7.

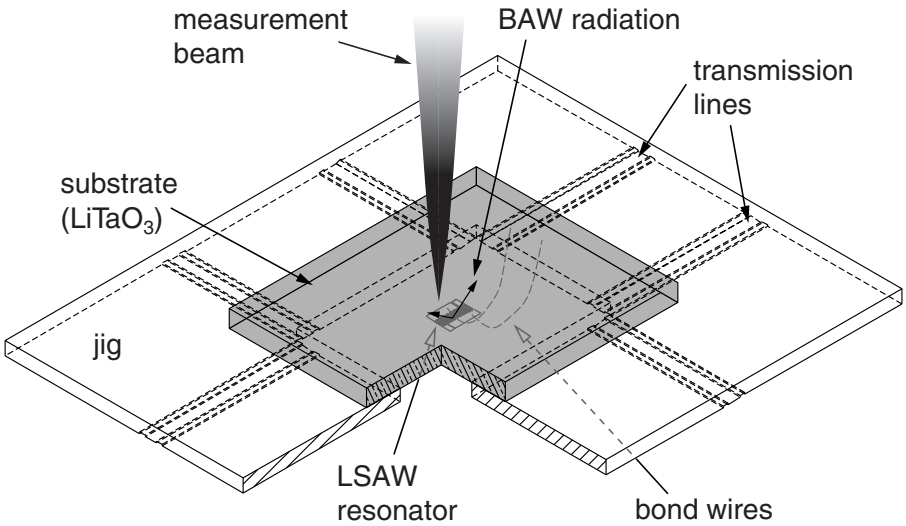

Figure 4.6: Schematic of the sample construction used for measuring the bulk-acoustic wave reflection patterns at the bottom surface of the substrate. By flipping the assembly, interferometric measurements can be performed on the top side.

The test resonator employed is a synchronous LSAW resonator on 36° YX-cut $LiTaO_3$ substrate. The sample is the one studied also in Paper V (selected scans from the topside are displayed in Fig 4.2). In the bottom scans shown in Fig 4.7, the resonator is located at the center of the image, but on the opposite side of the substrate. Each scan consists of 762 000 individual measurement points and the scanning step sizes are 1.65 μm in the transverse direction and 5.5 μm in the longitudinal direction. The time required for each scan was little over 22 hours resulting in a scanning speed of ∼34300 points/hour. Maximum scanning speed is not achieved due to the relatively long scanning step sizes. The long-term stability of the interferometer is sufficient for such long-running scans, though beam alignment is definitely advisable between scans.

At frequencies 906 MHz (resonance) and 934 MHz (antiresonance), the slow shear bulk acoustic waves (SSBAWs) arriving at the substrate bottom are visible as two patterns of high amplitude. The second arrivals of bulk acoustic waves at the substrate bottom after reflections from the top surface, though possessing weaker amplitudes, are also visible at 906 and 934 MHz. The energy-flow angle into the substrate varies only slightly. A white dotted line with rectangular boxes is shown in Fig 4.7 to indicate the location of the first SSBAW reflection occurring on the right hand side.

Well above the stopband, at frequencies 970 MHz and 1 GHz, the images feature additional distinct patterns whose energy-flow angles strongly depend on the frequency, shown in Fig 4.7 with a white dotted line with ellipsoidal circles. They were identified as directly excited fast shear bulk acoustic waves (FSBAWs) arriving at the bottom. At 950 MHz, continuous and semiperiodic patterns appear, extending to the edges of the scanned area. Due to their larger propagation angle, these patterns have been identified as the first appearance of the backward eigenmode-coupled FSBAW. For higher frequencies, these FSBAW patterns consist of two small (parallel) spots. Two arrows have been added to Fig 4.7(i). They point to the two spots located on the right hand side. In addition, a white dotted line in Figs. 4.7(e)–(i) approximately follows the location of one of the patterns. Interestingly, backward eigenmode-coupled FSBAW occurs only at the reflectors. The periodic pattern at 950 MHz is assumed to be related to the finger structure. It is suggested in Paper VII that radiation from each individual reflector finger shows up as a separate pattern on the backside.

From the scans in Fig 4.7, the experimental energy-flow angles for each mode are calculated using the known substrate thickness (345 μm) and the location of each pattern on the substrate backside. It should be noted that the experimental values exhibit a small (∼1 MHz) downward frequency shift, due to the elevated temperature induced by the high input power used (21 dBm).

4.2.2 Theoretical Analysis

A periodic array of electrodes can radiate bulk acoustic waves via three different mechanisms: (i) direct excitation, (ii) eigenmode leakage and (iii) scattering into bulk acoustic waves.

Direct excitation: Since the period of the voltage applied across the structure is

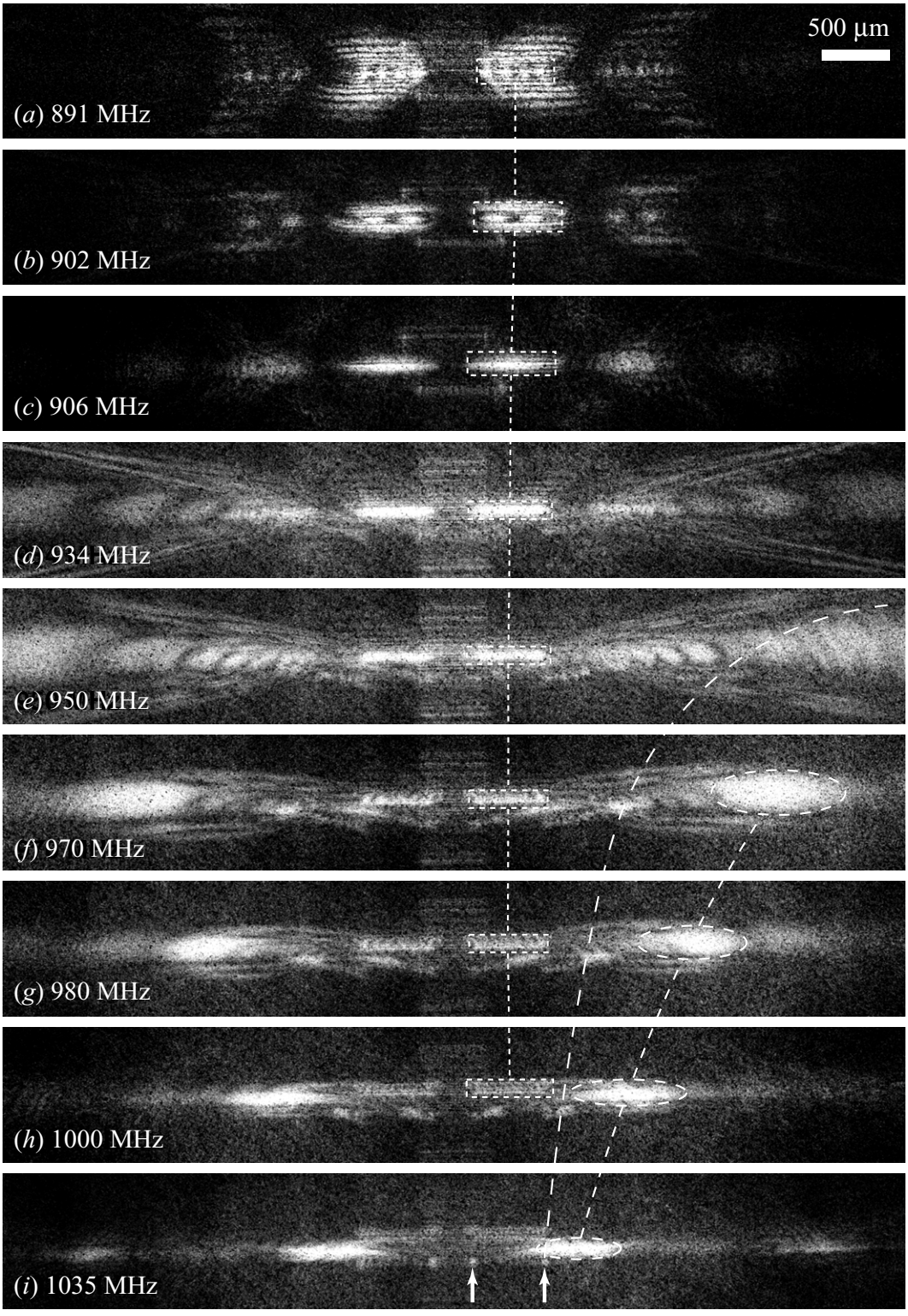

Figure 4.7: Measured bulk-acoustic wave reflection patterns at the bottom surface of the SAW substrate.

$\lambda_0 = 2p$, the resonator generates waves for which the x component of the wavevector is a multiple of $2\pi/\lambda_0 = \pi/p$. A bulk-acoustic wave mode i can be generated when the condition $k_i(\theta)\cos\theta = n\pi/p$ is fulfilled.

Eigenmode leakage and scattering into bulk acoustic waves: In addition to the directly excited waves, eigenmodes propagate in a SAW resonator to both directions. Owing to reflections from the electrodes, the Fourier decomposition of the eigenmodes contains components for which the x component of the wave vector is of the form $\pm k_{eig} + n2\pi/p$, where n is an integer. The eigenmodes can couple to the bulk acoustic waves, provided that the condition $k_i(\theta)\cos\theta = \pm k_{eig} + n2\pi/p$ is met. In practice, the cases $n = 0, -1$ are involved at the fundamental frequency. In the case $n = 0$, the eigenmode leaks into BAWs; for $n = -1$, the reflected eigenmode scatters into a BAW.

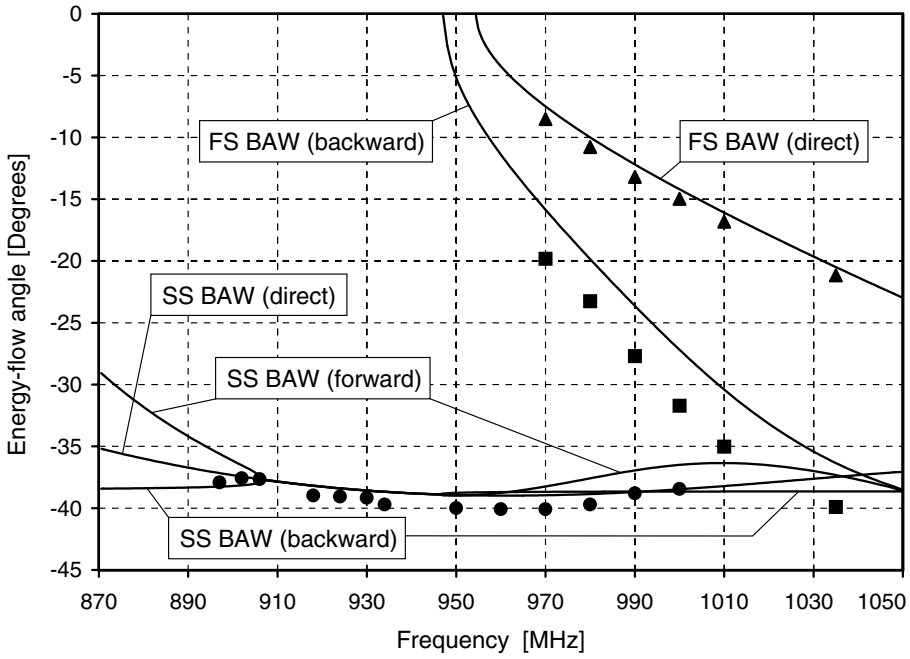

Figure 4.8: Measured (points) and calculated (continuous curves) values of the energy-flow angles for the various BAW radiation patterns.

For the LSAW resonator studied here, there occurs SSBAW radiation due to both of these mechanisms. The emission angles for the direct excitation of BAW can be calculated with help of Peach's method, see [199]. The computation of the leakage of the eigenmodes and the scattering is more involved and requires a self-consistent solution of the dispersion equation. Slowness along the surface as a function of frequency has been determined by applying Plessky's 2-parameter dispersion relation [200]. Thereafter, the Peach equation [199] along with data by Kovacs *et al.* [109] has been used to find the z-slowness and fields of those BAWs with the given surface slowness. Finally the Poynting vector for the x,z-slowness and fields have been computed and the angle of energy flow calculated from $\alpha = \arctan P_z/P_x$.

Simulated and measured results are shown in Fig 4.8. The threshold frequencies for the FSBAW (direct and backward) are explained since the x component of a bulk acoustic wave can obtain all values in the range $|(k_i)_x| \leq 2\pi f/(v_i)_x|_c$, where $(v_i)_x|_c^{-1}$ =max$[\cos\theta/v(\theta)]$. Hence a bulk acoustic wave mode i can be synchronously excited at all frequencies above the threshold value $(f_B)_i = (v_i)_x|_c/2p$. LSAW resonators usually operate at frequencies slightly below the threshold frequency for fast shear bulk acoustic waves. Hence the SSBAW is excited directly, while the FSBAW is only excited above the threshold frequency.

The minor discrepancies in Fig 4.8 between the calculated and experimental results are attributed to the approximations used in the computations, especially those concerning the backward eigenmode-coupled FSBAW.

5 Conclusions and Discussion

This Thesis focuses on laser-interferometric measurements of leaky surface acoustic waves (LSAW) on rotated Y-cut $LiTaO_3$. LSAW resonators form the basic operational blocks of impedance element surface acoustic wave filters which are commonly used in mobile phone front-end circuitry. The present work consists of (i) development of the homodyne Michelson interferometer setup and (ii) application of the interferometer to image and analyze acoustic phenomena in LSAW resonators on 36° YX-cut $LiTaO_3$ and 42° YX-cut $LiTaO_3$.

In the course of this work a homodyne Michelson interferometer was equipped with high-speed photodetector, high-precision motorized scanning stages, a piezo element for controlling the reference mirror as well as RF-isolation to suppress interference between the sample and the detection electronics. Furthermore, the complete setup was automated with the help of a computer and control software.

The system is capable of measuring surface waves with amplitudes on the order of a few picometers and wavelengths down to 2 micrometers. The optical setup features a spatial resolution better than one micrometer, and allows samples to be measured at a sufficient working distance to accommodate bond wires and package assemblies. The motorized stages can position the sample with submicron accuracy. The high sensitivity and good spatial resolution of the interferometer system combined with its capability to measure surface vibrations up to 2 GHz have proven it to be an effective analysis tool for surface acoustic wave devices. The computer control and data-storage schemes implemented into the imaging system facilitate two-dimensional automatically performed scans with a high number of scanning points (in the excess of million data points per measurement) and measuring speeds up to 50 000 points per hour. The interferometer setup is reported in Paper I.

Measurements performed on LSAW impedance element filters revealed an unexpected surface-wave amplitude field on top of the busbars. These measurements (Papers II and IV) showed that waves escaped outside the waveguide structure. Further measurements on a test resonator on $LiTaO_3$ revealed the frequency dependence and the antisymmetrical nature of the leakage. A model explaining the observed phenomena was developed [III] and simulations were performed to confirm that the observed leakage deteriorates the electrical performance of the resonator close to its resonance frequency [V]. A more detailed discussion on the modelling techniques used can be found in the PhD work of Julius Koskela [201]. The significance of the discovered effect is evident as two major SAW component manufactures have later published results on the topic as well as developed new device designs where measures have been taken to suppress the leakage mechanism [202, 203]. In addition at least one European SAW component manufacturer has implemented new designs which aim at eliminating the leakage.

In addition to the work on waveguide leakage, measurements on the BAW radi-

ation fields have been carried out and reported in Papers VI and VII. Radiation of bulk acoustic waves is inherent and one of the most significant loss mechanisms in LSAW resonators. Many analytic models as well as numerical simulations have been published on the subject. Many factors, e.g., the choice of the piezoelectric substrate material, crystal cut, and thickness of the electrodes, play a role for BAW radiation. These are introduced in more detail in [201]. Although theoretically determined parameters for small radiation losses are known and their values have been verified via electrical measurements, only few publications featuring direct measurements of the bulk radiation exist. By measuring the BAW radiation patterns on the backside of the crystal, both fast shear and slow shear bulk waves were shown to be present. Different coupling mechanisms, backscattering, and direct excitation were also identified. The results yield unique information on BAW radiation fields generated by a LSAW resonator on $LiTaO_3$.

Though providing valuable information which is impossible to obtain via electrical measurements alone, the homodyne interferometer described here has its limitations. Due to a difference in the reflectivities of the crystal surface and the metallized electrodes, the sensitivity of the interferometer varies for the crystal and metallized surfaces. The absolute surface vibration amplitude cannot be obtained without tedious calibration against a known reference. In practical measurements involving SAW devices such a procedure was never attempted. A further shortcoming, due to the selected electrical detection setup, is the fact that information on the phase of the acoustic vibrations is not obtained. Furthermore, the homodyne detection scheme is vulnerable to RF-crosstalk between the sample and the detection electronics.

To overcome these limitations a second scanning interferometer utilizing optical heterodyning is currently under development at the Materials Physics Laboratory of Helsinki University of Technology [204]. By using the laser wavelength as a fundamental reference, the setup provides an absolute amplitude, thus overcoming the issues concerning the different reflectivities and eliminating the need for calibration samples. The detection scheme also provides phase information and is not prone to direct RF-crosstalk between the sample and the detection electronics. Owing to the optical heterodyning, the setup is immune to optical path length variations which enables line scans and frequency sweeps. Both of these measurement modes can provide significant improvements to the overall measurement speed.

The applications for the heterodyne interferometer, and for optical imaging techniques in general, are manifold. Analysis of the existing device designs provides a plethora of future research topics. For example, quantitative measurements on the bulk acoustic radiation in LSAW devices would be valuable for a number of reasons. In addition, the development of mobile telecommunication applications towards higher operation frequencies requires new substrate materials and crystal cuts and wave types with high wave velocities. Direct optical measurements have served to characterize the acoustical properties of new materials and waves in the past and will probably do so in the future. Parameters important for device design such as wave velocity, attenuation, diffraction and reflection can all be obtained with the heterodyne probe.

In addition to offering advantages for the SAW technology, the direct measurement of the surface vibrations can greatly benefit the R&D work on devices based on thin-film bulk acoustic resonators (FBAR). Interferometric techniques have already been applied to analysis of FBARs [205–208]. Another emerging technique where interferometry can be applied is research of radio-frequency microelectromechanical systems (RF-MEMS) [209–211]. Finally, nonlinear effects in all of the above applications provide many challenging and interesting research topics.

In view of the results obtained in this Thesis and by other groups working in the field it is evident that optical imaging will continue to benefit both the scientific research on physics of surface and bulk acoustic waves and the industry driven development of SAW, BAW and RF-MEMS components.

References

[1] Lord Rayleigh,"On waves propagated along the plane surface of elastic solid", *Proc. London Math. Society* **17**, 4–11 (1885).

[2] R. M. White and F. W. Voltmer, "Direct piezoelectric coupling to surface elastic waves", *Appl. Phys. Lett.* **7**, 314–316 (1965).

[3] O. Ikata, T. Miyashita, T. Matsuda, T. Nishihara and Y. Satoh, "Development of low-loss band-pass filters using SAW resonators for portable telephones", *Proc. 1992 IEEE Ultrason. Symp.*, 111–115 (1992).

[4] O. Ikata, Y. Satoh, H. Uchishiba, H. Taniguchi, N. Hirasawa, K. Hashimoto and H. Ohmori, "Development of small antenna duplexer using SAW filters for handheld phones", *Proc. 1993 IEEE Ultrason. Symp.*, 111–114 (1993).

[5] M. Hikita, N. Shibagaki, T. Akagi and K. Sakiyama, "Design methodology and synthesis techniques for ladder-type SAW resonator coupled filters", *Proc. 1993 IEEE Ultrason. Symp.*, 15–24 (1993).

[6] M. Ueda, O. Kawachi, K. Hashimoto, O. Ikata and Y. Satoh, "Low loss ladder type SAW filter in the range of 300 to 400 MHz", *Proc. 1994 IEEE Ultrason. Symp.*, 143–146 (1994).

[7] J. Heighway, S. N. Kondratiev and V. P. Plessky, "Balanced bridge SAW impedance element filters", *Proc. 1994 IEEE Ultrason. Symp.*, 27–30 (1994).

[8] T. Morita, Y. Watanabe, M. Tanaka and Y. Nakazawa, "Wideband low loss double mode SAW filters", *Proc. 1992 IEEE Ultrason. Symp.*, 95–104 (1992).

[9] M. A. Sharif, C. Lambert, D. P. Chen and C. S. Hartmann, "Network coupled, high performance SAW resonator filters", *Proc. 1994 IEEE Ultrason. Symp.*, 135–138 (1994).

[10] European Patent Application EP0845858A2, "Surface acoustic wave device", Fujitsu Ltd, Kanagawa, Japan, M. Ueda, O. Kawachi, G. Endoh and Y. Fujiwara, 3rd June (1998).

[11] H. F. Tiersten and R. C. Smythe, "Guided acoustic surface wave filters", *Proc. 1975 IEEE Ultrason. Symp.*, 293–294 (1975).

[12] M. Tanaka, T. Morita, K. Ono and Y. Nakazawa, "Narrow bandpass filter using double-mode SAW resonators on quartz", *Proc. 38th Ann. Freq. Contr. Symp.*, 286–293 (1984).

[13] G. Martin, "Transversely coupled resonator filters", *Proc. 1999 IEEE Ultrason. Symp.*, 15–24 (1999).

[14] M. Lewis, "SAW filters employing interdigitated interdigital transducers", *Proc. 1982 IEEE Ultrason. Symp.*, 12–17 (1982).

[15] M. Hikita, T. Tabuchi, H. Kojima, A. Nakagoshi and Y. Kinoshita, "Low loss filter for antenna duplexer", *Proc. 1983 IEEE Ultrason. Symp.*, 77–82 (1983).

[16] E. P. Ippen, "Diffraction of light by surface acoustic waves", *Proc. of the IEEE* **55**, 248–249 (1967).

[17] A. Korpel, L. J. Laub and H. C. Sievering, "Measurement of acoustic surface wave propagation characteristics by reflected light", *Appl. Phys. Lett.* **10**, 295–297 (1967).

[18] J. Krokstad and L. O. Svaasand, "Scattering of light by ultrasonic surface waves in quartz", *Appl. Phys. Lett.* **11**, 155–157 (1967).

[19] H. A. Deferrari, R. A. Darby and F. A. Andrews, "Vibrational measurement by a laser interferometer", *J. Acoust. Soc. Am.* **42**, 982–990 (1967).

[20] W. G. Mayer, G. B. Lamers and D. C. Auth, "Interaction of light and ultrasonic surface waves", *J. Acoust. Soc. Am.* **42**, 1255–1257 (1967).

[21] D. C. Auth and W. G. Mayer, "Scattering of light reflected from acoustic surface waves in isotropic solids", *J. Appl. Phys.* **38**, 5138–5140 (1967).

[22] R. Adler, A. Korpel and P. Desmares, "An instrument for making surface waves visible", *IEEE Trans. SU* **15**, 157–161 (1968).

[23] R. L. Whitman, L. J. Laub and W. J. Bates, "Acoustic surface displacement measurements on wedge-shaped transducer using an optical probe technique", *IEEE Trans. SU* **15**, 366–369 (1968).

[24] E. Salzmann, T. Plieninger and K. Dransfeld, "Attenuation of elastic surface waves in quartz at frequencies of 316 MHz and 1047 MHz", *Appl. Phys. Lett.* **13**, 14–15 (1968).

[25] E. Salzmann and D. Weismann, "Optical detection of Rayleigh waves", *J. Appl. Phys.* **40**, 3408–3409 (1969).

[26] A. J. Slobodnik, Jr., "Microwave frequency acoustic surface wave propagation losses in $LiNbO_3$", *Appl. Phys. Lett.* **14**, 94–96 (1969).

[27] M. R. Serbyn and F. A. Andrews, "Measurement of the phase of vibrational displacement by a laser interferometer", *J. Acoust. Soc. Am.* **46**, 2–5 (1969).

[28] S. Sizgoric and A. A. Gundjian, "An optical homodyne technique for measurement of amplitude and phase of subangstrom ultrasonic vibrations", *Proc. of the IEEE* **57**, 1313–1314 (1969).

[29] E. A. Ash, R. M. De La Rue and R. F. Humphryes, "Microsound surface waveguides", *IEEE Trans. Microwave Theory Tech.* **17**, 882–892 (1969).

[30] B. H. Soffer, D. H. Close and M. E. Pedinoff, "An optical imaging method for direct observation and study of acoustic surface waves", *Appl. Phys. Lett.* **15**, 339–342 (1969).

[31] E. G. H. Lean, C. C. Tseng and C. G. Powell, "Optical probing of acoustic surface-wave harmonic generation", *Appl. Phys. Lett.* **16**, 32–35 (1970).

[32] E. G. Lean and C. C. Tseng, "Nonlinear effects in surface acoustic waves", *J. Appl. Phys.* **41**, 3912–3917 (1970).

[33] E. G. H. Lean and C. G. Powell, "Optical probing of surface acoustic waves", *Proc. of the IEEE* **58**, 1939–1947 (1970).

[34] B. A. Richardson and G. S. Kino, "Probing of elastic surface waves in piezoelectric media", *Appl. Phys. Lett.* **16**, 82–84 (1970).

[35] O. I. Diachok, R. J. Hallermeier and W. G. Mayer, "Measurement of ultrasonic surface wave velocity and absorptivity on single-crystal copper", *Appl. Phys. Lett.* **17**, 288–289 (1970).

[36] A. J. Slobodnik, Jr., "Microwave acoustic surface wave investigations using laser light deflection", *Proc. of the IEEE* **58**, 488–490 (1970).

[37] A. J. Slobodnik, Jr., "Nonlinear effects in microwave acoustic $LiNbO_3$ surface-wave delay lines", *J. Acoust. Soc. Am.* **48**, 203–210 (1970).

[38] A. J. Slobodnik, Jr., P. H. Carr and A. J. Budreau, "Microwave frequency acoustic surface-wave loss mechanisms on $LiNbO_3$", *J. Appl. Phys.* **41**, 4380–4387 (1970).

[39] R. V. Schmidt, "Optical probing of bulk waves present in acoustic surface wave delay lines", *Appl. Phys. Lett.* **17**, 369–371 (1970).

[40] R. L. Lawson, B. J. Hunsinger and F. Y. Cho, "Visualization of acoustic surface waves in an experimental Fabry-Perot interferometer", *Appl. Opt.* **9**, 2805–2807 (1970).

[41] G. Cambon, M. Rouzeyre and G. Simon, "Optical probing of surface Rayleigh waves", *Appl. Phys. Lett.* **18**, 295–298 (1971).

[42] E. G. Lean and C. G. Powell, "Nondestructive testing of thin films by harmonic generation of dispersive Rayleigh waves", *Appl. Phys. Lett.* **19**, 356–359 (1971).

[43] E. Bridoux, J. M. Rouvaen, C. Coussot and E. Dieulesaint, "Rayleigh-wave propagation on $Bi_{12}GeO_{20}$", *Appl. Phys. Lett.* **19**, 523–524 (1971).

[44] M. Zuliani and V. M. Ristic, "Visualization of acoustic radiation in $LiNbO_3$", *Phys. Lett.* **38A**, 87–88 (1972).

[45] A. J. DeVries and R. L. Miller, "Optical measurement of surface-wave scatter losses in piezoelectric ceramics", *Appl. Phys. Lett.* **20**, 210–212 (1972).

[46] R. V. Schmidt, "Excitation of shear elastic waves by an interdigital transducer operated at its surface-wave center frequency", *J. Appl. Phys.* **43**, 2498–2501 (1972).

[47] V. M. Ristic, M. Zuliani, G. Stegeman and P. Vella, "Probing of acoustic shear wave radiation in surface wave devices", *Appl. Phys. Lett.* **21**, 85–87 (1972).

[48] A. J. Slobodnik, Jr. and A. J. Budreau, "Acoustic surface wave loss mechanisms on $Bi_{12}GeO_{20}$ at microwave frequencies", *J. Appl. Phys.* **43**, 3278–3283 (1972).

[49] E. L. Adler, E. Bridoux, G. Coussot and E. Dieulesaint, "Harmonic generation of acoustic surface waves in $Bi_{12}GeO_{20}$ and $LiNbO_3$", *IEEE Trans. SU* **20**, 13–16 (1973).

[50] G. Coussot, "Rayleigh wave guidance on $LiNbO_3$", *Appl. Phys. Lett.* **22**, 432–433 (1973).

[51] T. L. Szabo, "Surface acoustic wave losses of thin-film gratings", *Appl. Phys. Lett.* **22**, 484–486 (1973).

[52] T. L. Szabo and A. J. Slobodnik, Jr., "The effect of diffraction on the design of acoustic surface wave devices", *IEEE Trans. SU* **20**, 240–251 (1973).

[53] P. J. Vella, G. I. A. Stegeman, M. Zuliani and V. M. Ristic, "High-resolution spectroscopy for optical probing of continuously generated surface acoustic waves", *J. Appl. Phys.* **44**, 1–4 (1973).

[54] P. J. Vella and G. I. A. Stegeman, "Optical probing of surface acoustic wave generation under interdigital transducers", *Appl. Phys. Lett.* **22**, 480–481 (1973).

[55] P. J. Vella, W. S. Goruk and G. I. Stegeman, "Surface wave generation by interdigital transducer", *Proc. 1973 IEEE Ultrason. Symp.*, 107–111 (1973).

[56] P. J. Vella and G. I. A. Stegeman, "Parametric coupling of bulk acoustic waves at surface interdigital transducers", *Appl. Phys. Lett.* **23**, 296–297 (1973).

[57] A. J. Slobodnik, Jr. and T. L. Szabo, "Minimal diffraction cuts for acoustic surface wave propagation on $Bi_{12}GeO_{20}$", *J. Appl. Phys.* **44**, 2937–2941 (1973).

[58] C. H. Palmer, "Ultrasonic surface wave detection by optical interferometry", *J. Acoust. Soc. Am.* **53**, 948–949 (1973).

[59] M. J. J. Zuliani, V. M. Ristic, P. J. Vella and G. I. A. Stegeman, "Probing of surface acoustic wave devices with large-diameter laser beam", *J. Appl. Phys.* **44**, 2964–2970 (1973).

[60] W. S. Goruk, P. J. Vella and G. I. A. Stegeman, "Visualization of inverse phase velocity surfaces of bulk and surface acoustic waves", *Phys. Lett.* **45A**, 357–358 (1973).

[61] P. J. Vella, W. S. Goruk and G. I. Stegeman, "Bulk wave generation by surface interdigital transducers operating near resonance", *Appl. Phys. Lett.* **24**, 165–167 (1974).

[62] T. E. Parker, "A new technique for a simple phase-sensitive laser probe", *Proc. 1974 IEEE Ultrason. Symp.*, 365–368 (1974).

[63] E. Bridoux, J. M. Rouvaen, M. Moriamez, R. Torguet and P. Hartemann, "Optoacoustic testing of microsound devices", *J. Appl. Phys.* **45**, 5156–5159 (1974).

[64] G. Coussot, "Nonlinear interactions in guided Rayleigh waves", *Appl. Phys. Lett.* **24**, 531–533 (1974).

[65] Y. Nakagawa, K. Yamanouchi and K. Shibayama, "Control of nonlinear effects in acoustic surface waves", *J. Appl. Phys.* **45**, 2817–2822 (1974).

[66] L. A. Coldren, "Rayleigh wave guidance using anisotropic topographic structures", *Appl. Phys. Lett.* **25**, 367–370 (1974).

[67] A. Alippi, A. Palma, L. Palmieri and G. Socino, "Determination of coupling coefficient in second harmonic generation of acoustic surface waves", *J. Appl. Phys.* **45**, 4347–4349 (1974).

[68] R. W. Weinert, P. R. Emtage, J. de Klerk and M. R. Daniel, "Are unexpected bulk waves produced by surface wave transducers?", *Appl. Phys. Lett.* **25**, 127–128 (1974).

[69] W. S. Goruk, P. J. Vella, G. I. Stegeman and V. M. Ristic, "An exponential coupling theory for interdigital transducers", *Proc. 1974 IEEE Ultrason. Symp.*, 402–405 (1974).

[70] S. Shiokawa, M. Ueda, T. Moriizumi, T. Yasuda and T. Sato, "Frequency-translated holography for the observation of surface acoustic waves", *Jpn. J. Appl. Phys.* **13**, 1907–1908 (1974).

[71] B. H. Nall, "Time and space resolution of bulk acoustic waves generated concomitantly with Rayleigh surface waves by an interdigital transducer", *J. Appl. Phys.* **46**, 1884–1892 (1975).

[72] W. S. Goruk and G. I. Stegeman, "Surface acoustic waves at a free-metallized interface", *Phys. Lett.* **53A**, 63–64 (1975).

[73] S. Shiokawa, M. Ueda, T. Moriizumi, T. Yasuda and T. Sato, "Observation and study of SAW by holographic technique", *Proc. of the IEEE* **63**, 1257–1258 (1975).

[74] S. Shiokawa, T. Moriizumi and T. Yasuda, "Study of SAW propagation characteristics by frequency-translated holography", *Appl. Phys. Lett.* **27**, 419–420 (1975).

[75] T. Chiba and Y. Togami, "Observation of bulk waves in surface acoustic wave device by frequency-shift holography", *Appl. Phys. Lett.* **29**, 793–795 (1976).

[76] P. J. Vella, G. I. Stegeman and V. M. Ristic, "Surface-wave harmonic generation on y-z, x-z, and $41\frac{1}{2}$-x lithium niobate", *J. Appl. Phys.* **48**, 82–85 (1977).

[77] A. Alippi, A. Palma, L. Palmieri and G. Socino, "Phase and amplitude relations between fundamental and second harmonic acoustic surface waves on SiO_2 and $LiNbO_3$", *J. Appl. Phys.* **48**, 2182–2190 (1977).

[78] C. H. Palmer, R. O. Claus and S. Fick, "Ultrasonic wave measurement by differential interferometry", *Appl. Opt.* **16**, 1849–1856 (1977).

[79] D. Murray and E. Ash, "Precision measurement of SAW velocities", *Proc. 1977 IEEE Ultrason. Symp.*, 823–826 (1977).

[80] R. M. De La Rue, "Heterodyne optical probing of surface acoustic waves in partial standing wave situation", *IEEE Trans. SU* **24**, 407–411 (1977).

[81] A. Alippi, A. Palma, L. Palmieri, G. Socino and E. Verona, "Visualization of field patterns in surface acoustic wave multistrip structures", *IEEE Trans. SU* **24**, 411–414 (1977).

[82] W. S. Goruk and G. I. Stegeman, "Surface to bulk mode conversion at interfaces on y-z $LiNbO_3$", *Appl. Phys. Lett.* **32**, 265–266 (1978).

[83] Y. Togami and T. Chiba, "Observation of bulk waves and surface waves through side planes of several cuts of $LiNbO_3$ SAW devices", *J. Appl. Phys.* **49**, 3587–3589 (1978).

[84] H. Engan, "Phase sensitive laser probe for high-frequency surface acoustic wave measurements", *IEEE Trans. SU* **25**, 372–377 (1978).

[85] T. Chiba, "SAW filters as applied to group-delay equalizer in television rebroadcast transmitters", *Proc. 1979 IEEE Ultrason. Symp.*, 545–549 (1979).

[86] W. S. Goruk and G. I. Stegeman, "Surface-wave reflection phenomena at interfaces on y-z $LiNbO_3$", *J. Appl. Phys.* **50**, 6719–6728 (1979).

[87] W. S. Goruk and G. I. Stegeman, "Acousto-optic measurement of bulk wave generation by interdigital transducers excited at SAW resonance", *J. Appl. Phys.* **50**, 6729–6732 (1979).

[88] R. L. Whitman and A. Korpel, "Probing of acoustic surface perturbations by coherent light", *Appl. Opt.* **8**, 370–379 (1969).

[89] R. M. White, "Surface elastic waves", *Proc. of the IEEE* **58**, 1238–1276 (1970).

[90] R. M. De La Rue, R. F. Humphryes, I. M. Mason and E. A. Ash, "Acoustic-surface-wave amplitude and phase measurements using laser probes", *Proc. of the IEE* **119**, 117–126 (1972).

[91] E. G. Lean, "Interaction of light and acoustic surface waves", *Progress in Optics* **XI** (ed. E. Wolf), 123–166 (North-Holland, 1973).

[92] G. I. Stegeman, "Optical probing of surface waves and surface wave devices", *IEEE Trans. SU* **23**, 33–63 (1976).

[93] J.-P. Monchalin, "Optical detection of ultrasound", *IEEE Trans. UFFC* **33**, 485–499 (1986).

[94] H. Sontag and A. C. Tam, "Optical detection of nanosecond acoustic pulses", *IEEE Trans. UFFC* **33**, 500–506 (1986).

[95] G. S. Kino, J. Fanton and B. T. Khuri-Yakub, "Optical measurements of acoustic and photoacoustic effects", *Proc. 1986 IEEE Ultrason. Symp.*, 505–514 (1986).

[96] J. W. Wagner, "Optical detection of ultrasound", *Physical Acoustics* **XIX** (eds. R. N. Thurston and A. D. Pierce), 201–266 (Academic Press, 1990).

[97] C. B. Scruby and L. E. Drain, *Laser Ultrasonics* (Adam Hilger, 1990).

[98] D. Royer and E. Dieulesaint, *Elastic waves in Solids II*, 157–233 (Springer, 2000).

[99] A. Aharoni and K. M. Jassby, "Monitoring surface properties of solids by laser-based SAW time-of-flight measurements", *IEEE Trans. UFFC* **33**, 250–256 (1986).

[100] W. D. Hunt, R. L. Miller and B. J. Hunsinger, "Slowness surface measurements for zero and five degree [100]-cut GaAs", *Proc. 1986 IEEE Ultrason. Symp.*, 451–456 (1986).

[101] W. D. Hunt, R. L. Miller and B. J. Hunsinger, "Slowness surface measurements for zero- and five-degree [100]-cut GaAs", *J. Appl. Phys.* **60**, 3532–3538 (1986).

[102] P. Cielo and C. K. Jen, "Laser generation of convergent acoustic waves and applications to materials evaluation", *Proc. 1986 IEEE Ultrason. Symp.*, 515–526 (1986).

[103] S. Jen, C. S. Hartmann and M. A. Domalewski, "Propagation of surface acoustic waves generated by slanted transducers: A laser probe study", *Proc. 1987 IEEE Ultrason. Symp.*, 271–277 (1987).

[104] M. Anhorn, H. E. Engan and A. Rønnekleiv, "New SAW velocity measurements on Y-cut $LiNbO_3$", *Proc. 1987 IEEE Ultrason. Symp.*, 279–284 (1987).

[105] W. D. Hunt and B. J. Hunsinger, "Experimental technique for the determination of surface acoustic wave grating impedance and velocity perturbations", *J. Appl. Phys.* **64**, 4347–4354 (1988).

[106] M. Anhorn and H. E. Engan, "SAW velocities in X-cut $LiTaO_3$", *Proc. 1989 IEEE Ultrason. Symp.*, 363–366 (1989).

[107] V. E. Steel, W. D. Hunt, M. A. Emanuel, J. J. Coleman and B. J. Hunsinger, "Surface acoustic wave properties of aluminum gallium arsenide", *J. Appl. Phys.* **66**, 90–96 (1989).

[108] A. Ginter and G. Sölkner, "Phase accurate optical probing of surface acoustic waves", *Appl. Phys. Lett.* **56**, 2295–2297 (1990).

[109] G. Kovacs, M. Anhorn, H. E. Engan, G. Visintini and C. C. W. Ruppel "Improved material constants for $LiNbO_3$ and $LiTaO_3$", *Proc. 1990 IEEE Ultrason. Symp.*, 435–438 (1990).

[110] A. Neubrand and P. Hess, "Laser generation and detection of surface acoustic waves: Elastic properties of surface layers", *J. Appl. Phys.* **71**, 227–238 (1992).

[111] V. M. Bright, Y. Kim and W. D. Hunt, "Study of surface acoustic waves on the {110} plane of gallium arsenide", *J. Appl. Phys.* **71**, 597–605 (1992).

[112] S. Jen and M. A. Domalewski, "Techniques for SAW device investigation using a high-performance phase-sensitive laser probe", *Proc. 1992 IEEE Ultrason. Symp.*, 433–436 (1992).

[113] Y. Kim, W. D. Hunt, Y. Liu and C.-K. Jen, "Velocity surface measurements for ZnO films over {001}-cut GaAs", *Proc. 1993 IEEE Ultrason. Symp.*, 243–248 (1993).

[114] R. Weigel, A. Holm, P. Russer, W. Ruile and G. Sölkner, "Accurate optical measurement of surface acoustic wave phase velocity", *Proc. 1993 IEEE Ultrason. Symp.*, 319–322 (1993).

[115] H. Nishino, Y. Tsukuhara, Y. Nagata, T. Koda and K. Yamanaka, "Optical probe detection of high-frequency surface acoustic waves generated by phase velocity scanning of laser interference fringes", *Jpn. J. Appl. Phys.* **33**, 3260–3264 (1994).

[116] H. Coufal, K. Meyer, R. K. Grygier, P. Hess and A. Neubrand, "Precision measurement of the surface acoustic wave velocity on silicon single crystals using optical excitation and detection", *J. Acoust. Soc. Am.* **95**, 1158–1160 (1994).

[117] Y. Kim, W. D. Hunt, Y. Liu and C.-K. Jen, "Surface acoustic wave properties of ZnO films on {001}-cut ⟨110⟩-propagating GaAs substrates", *J. Appl. Phys.* **75**, 7299–7303 (1994).

[118] Y. Kim, W. D. Hunt, Y. Liu and C.-K. Jen, "Velocity surface measurements for ZnO films over {001}-cut GaAs", *J. Appl. Phys.* **76**, 1455–1461 (1994).

[119] K. Yamanaka, Y. Nagata, S. Nakano, T. Koda, H. Nishino, Y. Tsukahara, H. Cho, M. Inaba and A. Satoh, "SAW velocity measurement of crystals and thin films by the phase velocity scanning of interference fringes", *IEEE Trans. UFFC* **42**, 381–386 (1995).

[120] M. G. Somekh, M. Liu, H. P. Ho and C. W. See, "An accurate non-contacting laser based system for surface wave velocity measurement", *Meas. Sci. Technol.* **6**, 1329–1337 (1995).

[121] H. Cho, H. Sato, M. Takemoto, A. Sato and K. Yamanaka, "Surface acoustic wave velocity and attenuation dispersion measurement by phase velocity scanning of laser interference fringes", *Jpn. J. Appl. Phys.* **35**, 3062–3065 (1996).

[122] C. Desmet, V. Gusev, W. Lauriks, C. Glorieux and J. Thoen, "Laser-induced thermoelastic excitation of Scholte waves", *Appl. Phys. Lett.* **68**, 2939–2941 (1996).

[123] A. Holm, R. Weigel, P. Russer and W. Ruile, "A laser probing system for characterization of SAW propagation on $LiNbO_3$, $LiTaO_3$, and quartz", *IEEE 1996 Int. Microwave Symp. Digest*, 1541–1544 (1996).

[124] C. Desmet, V. Gusev, W. Lauriks, C. Glorieux and J. Thoen, "All-optical excitation and detection of leaky Rayleigh waves", *Opt. Lett.* **22**, 69–71 (1997).

[125] K. Yamanaka, "Precise measurement in laser ultrasonics by phase velocity scanning of interference fringes", *Jpn. J. Appl. Phys.* **36**, 2939–2945 (1997).

[126] A. Holm, P. Wallner, W. Ruile and R. Weigel, "High-resolution optical probing of SAW and leaky SAW structures", *Proc. 1997 IEEE Ultrason. Symp.*, 153–156 (1997).

[127] Y.-C. Shen and P. Hess, "Real-time detection of laser-induced transient gratings and surface acoustic wave pulses with a Michelson interferometer", *J. Appl. Phys.* **82**, 4758–4762 (1997).

[128] Y. Hong, S. D. Sharples, M. Clark and M. G. Somekh, "Rapid measurement of surface acoustic wave velocity on single crystals using an all-optical adaptive scanning acoustic microscope", *Appl. Phys. Lett.* **83**, 3260–3262 (2003).

[129] H. Engan, "Laser probing of SAW convolver waveguide loss", *IEEE Trans. SU* **30**, 321–323 (1983).

[130] S. Jen and C. S. Hartmann, "An improved model for chirped slanted SAW devices", *Proc. 1989 IEEE Ultrason. Symp.*, 7–14 (1989).

[131] D. E. L. Vaughan, K. Doughty and K. H. Cameron, "Surface acoustic wave probe using lensed optical fibers", *Proc. 1991 IEEE Ultrason. Symp.*, 431–434 (1991).

[132] T. Yoshimine, H. Katoh, T. Igari, V. G. Kavalerov, M. Inoue and T. Fujii, "Reconstruction of three-dimensional images of surface acoustic waves by means of computer-controlled laser probe", *Jpn. J. Appl. Phys.* **33**, 3166–3169 (1994).

[133] V. Kavalerov, H. Katoh, N. Kasay, M. Inoue and T. Fujii, "Experimental studies on nonlinear dispersive surface acoustic waves for solitons", *Jpn. J. Appl. Phys.* **34**, 2653–2659 (1995).

[134] V. Kavalerov, H. Katoh, N. Kasay, M. Inoue and T. Fujii, "Phase sensitive optical probe for surface acoustic wave soliton investigation", *Jpn. J. Appl. Phys.* **35**, 3070–3074 (1996).

[135] V. Kavalerov, T. Fujii and M. Inoue, "Observation of highly nonlinear surface-acoustic waves on single crystal lithium-niobate plates by means of an optical sampling probe", *J. Appl. Phys.* **87**, 907–913 (2000).

[136] R. L. Jungerman, J. E. Bowers, J. B. Green and G. S. Kino, "Fiber optic laser probe for acoustic wave measurements", *Appl. Phys. Lett.* **40**, 313–315 (1982).

[137] H. Engan, T. Myrtveit and J. O. Askautrud, "All-fiber acousto-optic frequency shifter excited by focused surface acoustic waves", *Opt. Lett.* **16**, 24–26 (1991).

[138] M. Liu, H. P. Ho, M. G. Somekh and J. M. R. Weaver, "Noncontacting optical generation of focused surface acoustic waves using a customised zoneplate", *Elect. Lett.* **31**, 264–265 (1995).

[139] R. K. Ing, M. Fink and O. Casula, "Self-focusing Rayleigh wave using time reversal mirror", *Appl. Phys. Lett.* **68**, 161–163 (1996).

[140] M. Clark, F. Linnane, S. D. Sharples and M. G. Somekh, "Frequency control in laser ultrasound with computer generated holography" *Appl. Phys. Lett.* **72**, 1963–1965 (1998).

[141] M. Clark, S. D. Sharples and M. G. Somekh, "Fast laser generated Rayleigh wave scanning microscope", *Proc. 1998 IEEE Ultrason. Symp.*, 1317–1320 (1998).

[142] M. Clark, S. D. Sharples, M. G. Somekh and A. S. Leitch, "Non-contacting holographic surface acoustic wave microscope", *Elect. Lett.* **35**, 346–347 (1999).

[143] M. Clark, S. D. Sharples and M. G. Somekh, "Noncontact continuous wave-front/diffractive acoustic elements for Rayleigh wave control", *Appl. Phys. Lett.* **74**, 3604–3606 (1999).

[144] M. M. de Lima, Jr., F. Alsina, W. Seidel and P. V. Santos, "Focusing of surface-acoustic-wave fields on (100) GaAs surfaces", *J. Appl. Phys.* **94**, 7848–7855 (2003).

[145] D. Clorennec and D. Royer, "Investigation of surface acoustic wave propagation on a sphere using laser ultrasonics", *Appl. Phys. Lett.* **85**, 2435–2437 (2004).

[146] J. E. Bowers, R. L. Jungerman, B. T. Khuri-Yakub and G. S. Kino, "An all fiber-optic sensor for surface acoustic wave measurements", *J. Lightwave Tech.* **1**, 429–436 (1983).

[147] W. D. Hunt and B. J. Hunsinger, "A precise angular spectrum of plane-waves diffraction theory for leaky wave materials", *J. Appl. Phys.* **64**, 1027–1032 (1988).

[148] P. Kessler, G. Sölkner and K. Ch. Wagner, "Imaging of the wave field of surface acoustic wave devices", *Proc. 1991 IEEE Ultrason. Symp.*, 27–30 (1991).

[149] H. Yatsuda, S. Kamiseki and T. Chiba, "Calculation and optical measurement of SAW diffraction pattern of slanted finger SAW filters on YZ $LiNbO_3$ and 128YX $LiNbO_3$", *Proc. 2001 IEEE Ultrason. Symp.*, 13–17 (2001).

[150] T. Chiba, "Optical measurement and numerical analysis of SAW propagation at dispersive delay line on Y-Z $LiNbO_3$ substrate", *Proc. 2003 IEEE Ultrason. Symp.*, 1718–1721 (2003).

[151] S. D. Sharples, M. Clark and M. G. Somekh, "Dynamic higher-order correction of acoustic aberration due to material microstructure", *Appl. Phys. Lett.* **81**, 2288–2290, (2002).

[152] W. S. Goruk, P. J. Vella and G. I. Stegeman, "Optical probing measurements of surface wave generation and reflection in interdigital transducers on $LiNbO_3$", *IEEE Trans. SU* **27**, 341–354 (1980).

[153] S. Jen and C. S. Hartmann, "Laser probe investigation of leaky surface waves on 41° and 64°–$LiNbO_3$", *Proc. 1994 IEEE Ultrason. Symp.*, 293–296 (1994).

[154] H. Engan, "A Phase sensitive laser probe for pulsed SAW measurements", *IEEE Trans. SU* **29**, 281–284 (1982).

[155] T. P. Cameron, W. D. Hunt, H. M. Liaw and F. S. Hickernell, "Waveguide-coupled resonator filters on AlN on Silicon", *Proc. 1994 IEEE Ultrason. Symp.*, 371–374 (1994).

[156] T. Cameron and W. D. Hunt, "Reflection characteristics of obliquely incident surface acoustic waves from groove and aluminum gratings on {100}-cut gallium arsenide", *J. Appl. Phys.* **84**, 2212–2218 (1998).

[157] R. L. Jungerman, B. T. Khuri-Yakub and G. S. Kino, "Optical probing of acoustic waves on rough surfaces", *J. Acoust. Soc. Am.* **73**, 1838–1841 (1983).

[158] C. S. Hartmann, V. P. Plessky and S. Jen, "112°-$LiTaO_3$ periodic waveguides", *Proc. 1995 IEEE Ultrason. Symp.*, 63–66 (1995).

[159] V. Kavalerov, N. Kasaya, M. Inoue and T. Fujii, "Optical probing of nonlinear SAW waveform", *Proc. 1996 IEEE Ultrason. Symp.*, 839–844 (1996).

[160] Y.-C. Shen, A. Lomonosov, A. Frass and P. Hess, "Excitation of higher harmonics in transient laser gratings by an ablative mechanism", *Appl. Phys. Lett.* **73**, 1640–1642 (1998).

[161] F. M. Fliegel, B. F. Hall and R. S. Wagers, "Laser probe analysis of slot filters for a channelized receiver", *Proc. 1982 IEEE Ultrason. Symp.*, 218–221 (1982).

[162] D. Royer and E. Dieulesaint, "Optical detection of sub-Angström transient mechanical displacements", *Proc. 1986 IEEE Ultrason. Symp.*, 527–530 (1986).

[163] G. Sölkner, A. Ginter and H.-P. Graßl, "Phase-preserving imaging of high frequency surface acoustic wave fields", *Mater. Sci. Eng.* **A122**, 43–46 (1989).

[164] H. E. Engan and A. Rønnekleiv, "Enhancement of SAW laser probe measurements by signal processing", *Proc. 1999 IEEE Ultrason. Symp.*, 217–220 (1999).

[165] S. Rooth, S. Bardal, T. Viken, Ø. Johansen and E. Halvorsen, "Laserprobe measurements of SAWs at 3 GHz on a free surface of rotated Y-cut quartz", *Proc. 2001 IEEE Ultrason. Symp.*, 201–205 (2001).

[166] M. M. de Lima, Jr., W. Seidel, H. Kostial and P. V. Santos, "Embedded interdigital transducers for high-frequency surface acoustic waves on GaAs", *J. Appl. Phys.* **96**, 3494–3500 (2004).

[167] H. Nishino, Y. Tsukuhara, H. Cho, Y. Nagata, T. Koda and K. Yamanaka, "Generation and directivity control of bulk acoustic waves by phase velocity scanning of laser interference fringes", *Jpn. J. Appl. Phys.* **34**, 2874–2878 (1995).

[168] H. Nishino, Y. Tsukuhara, H. Cho, H. Sato and K. Yamanaka, "Unidirectional bulk acoustic wave excitation by scanning interference fringes and its application to acoustical imagings", *Proc. 1995 IEEE Ultrason. Symp.*, 673–678 (1995).

[169] R. O. Claus, "Differential optical measurements of the bulk particle motion fields of a surface acoustic wave", *IEEE Trans. SU* **27**, 93–94 (1980).

[170] S. Jen and C. S. Hartmann, "Direct measurement of SAW dispersion relation by laser probe", *Proc. 1995 IEEE Ultrason. Symp.*, 201–204 (1995).

[171] W. D. Hunt, T. Cameron, J. C. B. Saw, Y. Kim and M. S. Suthers, "Mode profiles in waveguide-coupled resonators", *Proc. 1992 IEEE Ultrason. Symp.*, 45–50 (1992).

[172] W. D. Hunt, T. Cameron, J. C. B. Saw, Y. Kim and M. S. Suthers, "Mode profiles in waveguide-coupled resonators", *J. Appl. Phys.* **74**, 4886–4893 (1993).

[173] C. S. Hartmann, B. P. Abbott, S. Jen and D. P. Chen, "Distortion of transverse mode symmetry in SAW transversely coupled resonators due to natural SPUDT effects", *Proc. 1994 IEEE Ultrason. Symp.*, 71–74 (1994).

[174] D. P. Chen, S. Jen and C. S. Hartmann, "Resonant modes in coupled resonator filters and the unique equivalent circuit representation", *Proc. 1995 IEEE Ultrason. Symp.*, 59–62 (1995).

[175] S. Jen and C. S. Hartmann, "Recent advances in SAW laser probe", *Proc. 1996 IEEE Ultrason. Symp.*, 33–36 (1996).

[176] S. Chamaly, R. Lardat, T. Pastureaud, P. Dufilie, W. Steichen, O. Holmgren, M. Kuitunen, J. V. Knuuttila and M. M. Salomaa, "SAW device analysis using a combination of FEM/BEM calculations and scanning interferometer measurements", *Proc. 2003 IEEE Ultrason. Symp.*, 294–298 (2003).

[177] S. Jen and C. S. Hartmann, "An improved propagation model for chirped slanted SAW devices", *Proc. 1988 IEEE Ultrason. Symp.*, 251–256 (1988).

[178] S. Jen, "Synthesis and performance of precision wideband slanted array compressors", *Proc. 1991 IEEE Ultrason. Symp.*, 37–49 (1991).

[179] J. V. Knuuttila, J. Koskela, P. T. Tikka, C. S. Hartmann, V. P. Plessky and M. M. Salomaa, "Asymmetric acoustic radiation in leaky SAW resonators on lithium tantalate", *Proc. 1999 IEEE Ultrason. Symp.*, 83–86 (1999).

[180] J. Koskela, J. V. Knuuttila, T. Makkonen, V. P. Plessky and M. M. Salomaa, "Acoustic loss mechanisms in leaky SAW resonators on lithium tantalate", *Proc. 2000 IEEE Ultrason. Symp.*, 209–213 (2000).

[181] A. Miyamoto, S. Wakana and A. Ito, "Novel optical observation technique for shear horizontal wave SAW resonator on 42°YX-cut lithium tantalate", *Proc. 2002 IEEE Ultrason. Symp.*, 86–89 (2002).

[182] S. Wakana, A. Miyamoto and A. Ito, "Backside observation technique for SAW distribution under electrodes", *Proc. 2003 IEEE Ultrason. Symp.*, 1714–1717 (2003).

[183] T. Makkonen, M. Kalo, V. P. Plessky, J. V. Knuuttila, W. Steichen and M. M. Salomaa, "Side radiation of Rayleigh waves from synchronous leaky SAW resonators", *Proc. 2003 IEEE Ultrason. Symp.*, 82–85 (2003).

[184] B. W. Busch and T. Gustafsson, "Thermal expansion and mean-square displacements of the Al(110) surface studied with medium-energy ion scattering", *Phys. Rev. B* **61**, 16097–16104 (2000).

[185] M. J. Hoskins and B. J. Hunsinger, "Optical probing of HF guided wave surface displacements with arbitrary profile", *IEEE Trans. SU* **27**, 103–111 (1980).

[186] D. A. Hutchins, D. E. Wilkins and G. Luke, "Electromagnetic acoustic transducers as wideband velocity sensors", *Appl. Phys. Lett.* **46**, 634–635 (1985).

[187] R. J. Dewhurst, C. Edwards and S. B. Palmer, "Noncontact detection of surface-breaking cracks using a laser acoustic source and an electromagnetic acoustic receiver", *Appl. Phys. Lett.* **49**, 374–376 (1986).

[188] M. Born and E. Wolf, *Principles of Optics* (Pergamon Press, 1980).

[189] H. H. Ou, N. Inose and N. Sakamoto, "Improvement of ladder-type SAW filter characteristics by reduction of inter-stage mismatching loss", *Proc. 1998 IEEE Ultrason. Symp.*, 97–102 (1998).

[190] V. P. Plessky, D. P. Chen and C. S. Hartmann, "'Patch' improvements to COM model for leaky waves", *Proc. 1994 IEEE Ultrason. Symp.*, 297–300 (1994).

[191] B. P. Abbot and K. Hashimoto, "A coupling-of-modes formalism for surface transverse wave devices", *Proc. 1995 IEEE Ultrason. Symp.*, 239–245 (1995).

[192] K. Hashimoto, G. Endoh and M. Yamaguchi, "Coupling-of-modes modelling for fast and precise simulation of leaky surface acoustic wave devices", *Proc. 1995 IEEE Ultrason. Symp.*, 251–256 (1995).

[193] V. Plessky and J. Koskela, "Coupling-of-modes analysis of SAW devices", *International Journal of High Speed Electronics and Systems* **10**, 867–947 (2000).

[194] J. Koskela, V. P. Plessky and M. M. Salomaa, "Theory for shear horizontal surface acoustic waves in finite synchronous resonators", *IEEE Trans. UFFC* **47**, 1550–1560 (2000).

[195] J. Knuuttila, P. Tikka, V. P. Plessky, T. Thorvaldsson and M. M. Salomaa, "Recent advances in laser-interferometric investigations of SAW devices", *Proc. 1997 IEEE Ultrason. Symp.*, 161–164 (1997).

[196] M. Feldmann and J. Hénaff, *Surface Acoustic Waves for Signal Processing*, (Artech House, 1989).

[197] M. P. da Cunha, "High velocity pseudo surface waves (HVPSAW): Further insight", *Proc. 1996 IEEE Ultrason. Symp.*, 97–106 (1996).

[198] C. S. Hartmann and V. P. Plessky, "Experimental measurements of propagation, attenuation, reflection and scattering of leaky waves in Al electrode gratings on 41°, 52° and 64°-$LiNbO_3$", *Proc. 1993 IEEE Ultrason. Symp.*, 1247–1250 (1993).

[199] R. C. Peach, "A general Green function analysis for SAW devices", *Proc. 1995 IEEE Ultrason. Symp.*, 221–225 (1995).

[200] V. P. Plessky, "A two parameter coupling-of-modes model for shear horizontal type SAW propagation in periodic gratings", *Proc. 1993 IEEE Ultrason. Symp.*, 195–200 (1993).

[201] J. Koskela, "Analysis and modeling of surface-acoustic wave resonators", PhD Thesis (Online), Materials Physics Laboratory, Helsinki University of Technology, Available: http://lib.hut.fi/Diss/2001/isbn9512253380/ (2001).

[202] T. Matsuda, J. Tsutsumi, S. Inoue, Y. Iwamoto, Y. Satoh, M. Ueda and O. Ikata, "High-frequency SAW duplexer with low-loss and steep cut-off characteristics", *Proc. 2002 IEEE Ultrason. Symp.*, 68–73 (2002).

[203] T. Shiba, S. Oosawa, J. Hamasaki, Y. Fujita and T. Chiba, "Low loss SAW double-mode structure suppressing spurious radiation", *Proc. 2004 IEEE Ultrason. Symp.*, 2008–2011 (2004).

[204] K. Kokkonen, J. V. Knuuttila, V. P. Plessky and M. M. Salomaa, "Phase-sensitive absolute-amplitude measurements of surface waves using heterodyne interferometry", *Proc. 2003 IEEE Ultrason. Symp.*, 1145–1148 (2003).

[205] J. E. Graebner, H. F. Safar, B. Barber, P. L. Gammel, J. Herbsommer, L. A. Fetter, J. Pastalan, H. A. Huggins and R. E .Miller, "Optical mapping of surface vibrations on a thin-film resonator near 2 GHz", *Proc. 2000 IEEE Ultrason. Symp.*, 635–638 (2000).

[206] J. E. Graebner, "Optical scanning interferometer for dynamic imaging of high-frequency surface motion", *Proc. 2000 IEEE Ultrason. Symp.*, 733–736 (2000).

[207] G. G. Fattinger and P. T. Tikka, "Laser measurements and simulations of FBAR dispersion relation", *IEEE 2001 Int. Microwave Symp. Digest*, 371–374 (2001).

[208] T. Makkonen, T. Pensala, J. Vartiainen, J. V. Knuuttila, J. Kaitila and M. M. Salomaa, "Estimating materials parameters in thin-film BAW resonators using measured dispersion curves", *IEEE Trans. UFFC* **51**, 43–51 (2004).

[209] A. Caronti, H. Majjad, S. Ballandras, G. Caliano, R. Carotenuto, A. Iula, V. Foglietti, and M. Pappalardo, "Vibration maps of capacitive micromachined ultrasonic transducers by laser interferometry", *IEEE Trans. UFFC* **49**, 289–292 (2002).

[210] J. F. Vignola, X. Liu, S. F. Morse, B. H. Houston, J. A. Bucaro, M. H. Marcus, D. M. Photiadis and L. Sekaric, "Characterization of silicon micro-oscillators by scanning laser vibrometry", *Rev. Sci. Instrum.* **73**, 3584–3588 (2002).

[211] O. Holmgren, K. Kokkonen, T. Mattila, V. Kaajakari, A. Oja, J. Kiihamäki, J. V. Knuuttila and M. M. Salomaa, "Imaging of in- and out-of-plane vibrations in micromechanical resonator", *Elect. Lett.* **41**, 121–122 (2005).

Abstracts of Publications I–VII

I A scanning homodyne Michelson interferometer is constructed for two-dimensional imaging of high-frequency surface acoustic wave (SAW) fields in SAW devices. The interferometer possesses a sensitivity of $\sim 10^{-5}\mathrm{nm}/\sqrt{\mathrm{Hz}}$, and it is capable of directly measuring SAW's with frequencies ranging from 0.5 MHz up to 1 GHz. The fast scheme used for locating the optimum operation point of the interferometer facilitates high measuring speeds, up to 50,000 points/h. The measured field image has a lateral resolution of better than 1 μm. The fully optical noninvasive scanning system can be applied to SAW device development and research, providing information on acoustic wave distribution that cannot be obtained by merely electrical measurements.

II The experimental discovery of a novel acoustic loss mechanism in SAW filters at RF frequencies is reported. The phenomenon is characterized by an unexpected spatial distribution of the surface-acoustic wave field. The observation and measurements were performed with a specially constructed scanning laser-interferometric probe. Current simulation methods and known phenomenological models applied to SAW resonators have no predictive ability to describe the discovered effect.

III We discuss an acoustic loss mechanism in surface-acoustic wave resonators on 36° YX-cut lithium tantalate substrate. Recent acoustic field scans performed with an optical Michelson interferometer reveal a spatially asymmetric acoustic field atop the busbars of a resonator, giving rise to acoustic beams which escape the resonator area and lead to undesired losses. Here, we link the phenomenon with the inherent crystalline anisotropy of the substrate: the shape of the slowness curves and the asymmetry of the polarization for leaky surface-acoustic waves, propagating at an angle with respect to the crystal X-axis.

IV Surface acoustic wave (SAW) impedance element antenna duplexers provide compact, high performance, front-end components apt for industrial fabrication. We describe investigations on the design and modeling of a compact ISM antenna duplexer fabricated on a 36° YX-cut $LiTaO_3$ substrate based on SAW impedance elements. In particular, we have performed 3-D modeling of the inductive and capacitive electromagnetic couplings caused by the package parasitics for the duplexer. The use of a 1:3 IDT structure for the reduction of the passband width is discussed. The frequency response of the duplexer is predicted with the help of circuit simulation; the modeling is refined by optimization of the model parameters to improve the fit between the measured and simulated responses. We also report scanning optical imaging of the acoustic field within the resonator structures with the help of laser interferometry; this provides insight into the loss mechanisms beyond that attainable in mere electric measurements.

V We discuss acoustic losses in synchronous leaky surface acoustic wave (LSAW) resonators on rotated Y-cut lithium tantalate ($LiTaO_3$) substrates. Laser probe measurements and theoretical models are employed to identify and characterize the radiation of leaky waves into the busbars of the resonator and the excitation of bulk acoustic waves. Escaping LSAWs lead to a significant increase in the conductance, typically occurring in the vicinity of the resonance and in the stopband, but they do not explain the experimentally observed deterioration of the electric response at the antiresonance. At frequencies above the stopband, the generation of fast shear bulk acoustic waves is the dominant loss mechanism.

VI The first direct experimental observation of bulk-acoustic wave radiation from a leaky surface-acoustic wave transducer, measured arriving at the backside of the piezoceramic substrate, is reported. A scanning laser-interferometric probe is used to map the spatial distribution of the bulk-wave radiation patterns on the substrate bottom. The different energy-flow angles into the substrate are obtained as functions of frequency and used to identify the corresponding bulk-wave modes arriving at the substrate bottom.

VII The bulk-acoustic conductance in low-loss surface-acoustic-wave filters utilizing leaky surface-acoustic waves is significant for the device operation. Here we directly measure the bulk acoustic wave radiation pattern on the backside of the piezoelectric substrate with the help of a scanning laser-interferometer probe. For the case studied, a leaky surface-acoustic wave resonator on 36°YX-$LiTaO_3$, a numerical calculation is carried out and the different bulk-wave modes arriving at the substrate bottom are identified by comparing the measured and computed energy-flow angles. The results are expected to lead to improved models for describing the operation of low-loss surface-acoustic-wave filters.